PRODUCTION OF SPONGE IRON IN A FLUIDIZED BED REACTOR

by

SHAILESH GUPTA

MME
995
1
UP
PRO

DEPARTMENT OF MATERIALS AND METALLURGICAL ENGINEERING

INDIAN INSTITUTE OF TECHNOLOGY KANPUR

MAY, 1995

PRODUCTION OF SPONGE IRON IN A FLUIDIZED BED REACTOR

A Thesis Submitted

In Partial Fulfilment of the Requirements

for the Degree of

MASTER OF TECHNOLOGY

by

SHAILESH GUPTA

to the

DEPARTMENT OF MATERIALS AND METALLURGICAL ENGINEERING

INDIAN INSTITUTE OF TECHNOLOGY, KANPUR

MAY, 1995

27 JUN 1996

CENTRAL LIBRARY
IIT KANPUR
Acc. No. A121705

MME-1995-M-GUP-PRO

A121705

DEDICATED TO

PROF. S.P.MEHROTRA

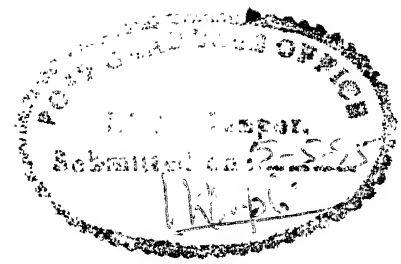

CERTIFICATE

This is to certify that the thesis entitled "PRODUCTION OF SPONGE IRON IN A FLUIDIZED BED REACTOR" by Mr. Shailesh Gupta has been carried out under my supervision, and this has not been submitted elsewhere for a degree.

Dated : May, 1995

(Dr. S.P.Mehrotra)

Professor

Department of Materials and Metallurgical Engineering

I.I.T. Kanpur

ACKNOWLEDGEMENT

I wish to express my sincere gratitude to Dr. S.P. Mehrotra for his inspiring supervision, encouragement and continued help throughout the project. I am very much grateful to him for his valuable suggestions and advice during the work. I am also thankful to him for giving me his time for discussion concerning my work.

I am grateful to Dr. N.K. Batra for his variety of assistance during my stay here.

I express my gratitude to my friends Rajeev, Akash, Anurag, Amit, Gagan, Arvind and Diwaker for reaching out their hands at crucial time.

I am highly thankful to Mr. D.P.Tripathi and Mr.A.Sharma whose efforts helped me in successful execution of the project.

A special thank is owed to Mr. K.S.Tripathi for his continuous support throughout the study of this work.

A special mention is due to Mr. V.P.Gupta for making beautiful tracings of figures with all his sincere effort and expertise.

Shailesh Gupta

TABLE OF CONTENTS

LIST OF FIGURES

LIST OF TABLES

ABSTRACT

In the present investigation some basic aspects of reduction of iron oxide with different reducing agent in a high temperature Fluidized Bed Reactor have been studied. With an objective to establish the feasibility of utilization of iron ore fines and coal fines (which otherwise discarded as a waste) directly for the production of sponge iron, four sets of experiments have been performed. In the first set hydrogen has been used as a reducing agent. In the second set several kinds of coal fines have been used as reducing agent with argon as a fluidizing medium. Hydrogen and methane mixture has been used in the third set of experiments while in the last set of experiments both coal and methane have been employed as reducing agent. The process variables which have been examined during the course of this investigation are temperature, reduction time and reducing agent.

From the chemical analysis of the final product it has been possible to determine percent reduction as function of time. Analysis of these data indicates that the reduction of iron ore with hydrogen or hydrogen and methane mixture gives the best results. However, it may not be economically viable to use these gases industrially in a country like India where both the gases are expensive. Results show that the reduction of iron ore with coal fines is meager even above 900^{o}C and that the rate of reduction is also low due to the solid-solid state reduction. Reduction with coal and methane, simultaneously used as reducing agent, however, shows good results.

Using the reduction data as a function of time reaction rate constant at various temperature is calculated. From this it has been possible to calculate the activation energies for various reducing agents using Arrhenius rate law. The overall activation energy for reduction of iron ore with hydrogen is found to be 14.85 kcal/mol while it is 24.47 kcal/mol when both hydrogen and methane are used. For the reduction with coal activation energy is found to be 40.0 kcal/mol where as for reduction with coal and methane it is 27.42 kcal/mol.

Characterization of Fluidized Bed Reactor product has been done using chemical and X-ray diffractograph analysis.

CHAPTER 1

INTRODUCTION

Large amounts of iron ore fines are produced during mining and comminution operations of iron ore and coal. It has been reported [1] that 19 mt of ore fines are produced out of 42 mt of ore mined annually in India. Similarly, 6 mt of coal fines are produced annually. For want of an appropriate process for directly treating these fines for production of iron, a large fraction of these is usually not utilized and discarded as a waste. Any process which is able to use these fines directly for production of iron, will not only provide a methodology of utilizing these fines but will also suggest an alternate method of producing iron. Among the various reduction processes now available on commercial scale (Table 1.1 c) only ESSO FIOR (Fluidised Iron Ore Reduction) and HIB (High Iron Briquetties) are based on direct reduction of iron ore fines. In these processes fines are reduced by reformed natural gas, and coal fines are not utilized. Clearly a process in which both the fines are utilized will be more desirable. So a process based on direct reduction of iron fines with coal fines and natural gas as reductants in a Fluidized Bed Reactor (FBR) may be of great interest.

1.1 A Fluidized Bed Reactor (FBR)

A FBR consists of a long cylinder with a distributor plate attached at its bottom. When a gas is passed through the distributor plate, at a low flow rate, gas merely percolates

through the bed without moving the solid particles. This corresponds to a fixed bed configuration. With an increase in gas flow rate particles move apart and a few are seen to vibrate and move about in a restricted region. This corresponds to an expanded bed situation. At a still higher velocity, a point is reached when the particles are just suspended in upward flowing gas. At this point, the drag force by the upward moving gas is equal to the weight of the bed. This stage is referred to as onset of fluidization, and the bed is considered to be just fluidized. This stage can be identified in a pressure drop versus velocity plot, schematically shown in Fig.A.1 in the APPENDIX A. After the onset of fluidization, the pressure drop across the bed becomes nearly constant.

Perhaps, the most important parameter in a FBR is the design of the distributor plate. Faulty design of the distributor plate in the reactor may cause a number of problems such as channeling, slugging, etc. Theoretical aspects of FBR design are discussed in detail in APPENDIX A.

In extractive metallurgy, the FBR are used for various gas solid reactions such as roasting, reduction, calcination, chlorination, [2-6] etc. Applications of FBR with reasonable success in hydro-metallurgical and electro-metallurgical processes have also been reported [6]. Besides these, FBR are also finding commercial applications in gasification of coal [7]. These applications are mainly due to a number of advantages associated with FBR.

1.1.1 Merits and Demerits of a FBR

It is well known that a FBR in general, is a highly efficient reactor. One may claim the following advantages.

a) Smooth liquid like flow of particle allows continuous, automatically controlled operation with ease of handling.
b) Requires less ore preparation.
c) Rapid mixing of solids leads to nearly isothermal condition in the reactor.
d) By choosing proper fluidizing conditions, it is possible to maintain gas composition very close to the equilibrium condition.
e) Excellent gas solid contact in the FBR leads to higher heat and mass transfer coefficients than in a fixed bed operating under comparable flow condition. Thus, the fluidized bed offers great advantage where highly exothermic or endothermic reactions are involved.

With normal fluidized bed reactors there are a few disadvantages as well.

a) Segregation and entrainment of particles can occur above the surface of fluidized bed.
b) It is not possible to control the reaction of each particle. It is only the average fraction reacted that can be controlled.
c) Solid particles in the size range 1 μm-640 μm can be treated in FBR but the best size range is in between 10 μm and 250 μm. Fine particles have a tendency to agglomerate and coarse ones result in non homogeneous fluidization and shock effects etc.

d) The volume of gas that can be passed through the reactor is a function of gas velocity that can be used without entraining the finely divided solids. In turn, the amount of material that can be treated is dependent on how much the fluidizing gas can be passed through the reactor.

1.2 Objective Of The Present Investigation

Carbon in sponge iron is of great operational and economic importance, particularly when it is to be used as a raw material for electric steelmaking. The amount of carbon in iron varies with the type of process and conditions of manufacture. It has been reported [8] that the iron oxide fines can be directly converted into iron carbide using carbonaceous material or hydrocarbon gases as reducing agent. Present investigation aims at an alternative direct reduction process producing carbon saturated sponge iron utilizing both coal fines and natural gas as reducing agents. The reduction kinetics of these experiments are compared with that of hydrogen reduction. Abundant literature is available on the reduction of iron ore with hydrogen. Since reduction is dependent upon ore characteristics, process design, etc, it has been planned to study the reduction kinetics of the same iron ore with hydrogen first, and use this data as reference to study the behaviour of other reducing agents. In the next series of experiments various combinations of reducing agents such as coal and methane, hydrogen and methane, etc have been investigated. It is speculated that an optimal process for our country would be the one in which iron ore is partially reduced with coal and partially with methane utilizing the advantages of gas solid reduction. The final product

of each experiment is chemically analyzed to estimate the metallic iron and total iron present. To identify the phases present in the FBR product, sponge iron samples have also been analyzed using X-ray diffraction.

Although abundant literature is available on reduction of iron ore with hydrogen, there is only a limited published literature on reduction of iron ore with carbon monoxide, coal and methane. Available literature has been reviewed in chapter 2. Design of FBR and preheater, experimental procedure and different experimental conditions are described in chapter 3. Results of all the experiments are presented and discussed in chapter 4 while chapter 5 incorporates conclusions of present investigation and suggestions for future study.

Table 1.1 a: Shaft furnace based industrial sponge iron making processes

Process	Charge type Size (mm)	Reductant used	Commercial plant at	Rated plant capacity (t/yr)
ARMCO	Pellet 5-20	Reformed Natural Gas	Houston USA	300,000
Midrex	Pellet 3-19	Reformed Natural Gas	South Carolina USA	400,000
NSC	Pellet -	Gasified Fuel Oil	NSC Japan	200,000
Purofer	Pellet 6-32	Reformed Natural Gas	Brazil	400,000

Table 1.1 b: Kiln based industrial sponge iron making processes

Process	Charge type Size (mm)	Reductant used	Commercial plant at	Rated plant capacity (t/yr)
SL/RN	Pellet 8-16	Solid Fuel Coke/Coal	Canada	385,000
Allis-Chalmers	Lump -	Liquified Carbon Natural Gas	Canada	260,000
Kawasaki	Pellet 10-15	Coke Solid Carbon	Japana	150,000
Krupp	Pellet <10	Solid Reducing agent	South Africa	150,000
SDR	Pellet -	Coke fines	Japan	200,000
SPM	Fines Slurry	Coke fines Coal	Japan	130,000
DRC	Pellet 5-20	Coke/Coal	Canada	65,000

Table 1.1 c: Fluidized bed reactor based sponge iron making processes

Process	Charge type Size (mm)	Reductant used	Commercial plant at	Rated plant capacity (t/yr)
ESSO FIOR	Fines	Reformed Natural Gas	Venezuela	440,000
HIB	Fines <1.65	Reformed Natural Gas	Venezuela	350,000
Novalfer	Fines	Reformed Natural Gas	France	18,000
H-Iron	Fines	Oil,Coke oven, Natural Gas	USA	36,000

CHAPTER 2

LITERATURE REVIEW

In this chapter, a brief review of literature on reduction kinetics of iron ore with hydrogen, coal and methane, respectively, has been presented in the first section. The form in which carbon may be present in sponge iron and its economic and operational importance have been discussed in section two. The commercial processes based on FBR are described in the last section of this chapter.

2.1 Reduction Kinetics Of Iron Ore

Iron ore reduction kinetics deals with the rate at which iron oxide is converted into metallic iron by removal of oxygen. For reduction to occur, the reductant must reach the reaction site and the product of the reaction must move away from it. The movements of reactants and products in this region are affected by several factors. The slowest of the kinetic steps is the rate controlling step. Some of the rate controlling steps in iron ore reduction are associated with the nature of the reaction system, i.e. FBR, rotary kiln, static bed, etc., determining how the contact between the reacting phases is stabilized while some of the steps are associated with the nature of the ore. The later determines the ease with which oxygen can be removed from the iron ore by a reductant. This property of the ore is referred to as its reducibility. The factors which determine the reducibility of an ore are particle size, particle size distribution, shape, density,

porosity, crystal structure and composition of the ore. All of these influence relative amount of reactive surface area of the ore exposed to the reductant. Joseph [9] carried out reducibility tests on several ores and concluded that the porosity of an iron ore particle is one of the most important factors controlling reducibility. The literature on iron ore reduction is too vast to be reviewed here, however, some important aspects are very briefly discussed below.

2.1.1 Reduction Kinetics Of Iron Ore With Hydrogen

Numerous fundamental investigations have been carried out in the past on kinetics of iron ore reduction by hydrogen [9-28]. However, there have been differences of opinion in literature as to whether the reduction of iron oxide is controlled by a diffusion process or by a reaction process. Udy and Lorig [10] believed that the reduction was probably controlled by diffusion of water vapor outward through a porous metal layer. Bogdandy and Janke [11] reported that the diffusion through pores was the rate controlling step. On the other hand Joseph [9] and Mckewan [12] indicated that the reaction was controlled at oxide metal interface. An important understanding of hemetite reduction kinetics with pure hydrogen is provided by Turkdogon and coworkers [13-15]. They suggested that the overall rate of reduction could be considered to fall between two limiting cases: (i) the uniform rate of reduction corresponding to chemical control, and (ii) an asymptotic approach towards shrinking core type behavior corresponding to diffusion control. Shrinking core model postulates that the reacted, partially reacted and unreacted

regions in a particle are separated by sharp interfaces.

According to Ezz [16] reduction of fine material proceeds in a step wise manner. The reduction starts at a high rate, decreasing gradually to a constant rate. For temperature below quadruple point the constancy begins at about 15% reduction while above quadruple point it starts at about 30% reduction. He also concluded that the rate of reduction of fluidized fine ore beds was mainly controlled by the rate of reducing gas supply. Hutching et al.[17] have also supported this view concluding that the rate of reduction was determined mainly by gas supply. According to them high temperature is probably advantageous in the final stages of reduction, while for earlier stages (up to 60-70% reduction) it may be desirable to save energy by operating at a lower temperature. A similar conclusion is reached by Feinmen also [18].

The reduction of iron ore by hydrogen and CO under increased pressure is investigated by Diepschlag [19]. He studied the reduction at pressure up to 7 atmosphere and found that the reduction rate increased as pressure was increased. This results was later confirmed by Tenen baum [20] and Mckewan [12], who found that increasing hydrogen partial pressure materially increase the reduction rates. The fact that there is a strong pressure dependence is an indication that the rate of reduction is controlled at oxide/metal interface rather than by diffusion through the reaction product layer.

All ore reduced commercially include a certain proportion of gaunge such as SiO_2, CaO, MgO, Al_2O_3 and S. Some improves the reducibility of the ore while others have a deleterious effect. Addition of CaO to iron oxide has an acceleration effect on reduction [21]. Comparison of time taken for 80% reduction of iron oxide sinters containing 2 to 10% CaO by hydrogen at 550-700^{o}C has shown a considerably accelerating effect on reduction. On the other hand addition of SiO_2 to iron oxide considerably lowers the reducibility due to formation of silicate during the process of reduction. The silicate formation results in lowering the porosity. Addition of CaO is also effective for preventing iron oxide from combining with SiO_2 especially when CaO/SiO_2 ratio is larger than 1.

Sakuraya et al.[22] studied the effect of internals placed inside the reactor. In case of beds without internals, gas bubbles tends to grow larger with increasing gas velocity. Gas bubbles are of smaller size and well dispersed in the case of beds with horizontal internals arranged in form of equilateral triangle in the model.

A number of investigators have performed the reduction of iron oxide with hydrogen under different experimental conditions and reported activation energy. Some of these are compiled in Table 2.1.

Table 2.1 : Activation energy data for the reduction of iron ore with hydrogen as a reducing agent

Material	Size(μm)	Temperature(K)	Act . Energy(kcal/mol)	Reference
Iron ore	47-246	708-1076	10.87-14.83	Koo et al [23]
Iron ore	15	1023-122	13.2-13.7	Ozawa et al [24]
Iron Oxide	600-2500	873-1323	14.9-15.3	Mckewan [12]
Wustite	50	794-963	16.82-17.25	Rao et al [25]
Hematite	400-2000	873-1598	14.5	Tohindi et al [27]
Magnetite	89	507-893	18.11-19.05	Rao et al [26]

2.1.2 Reduction Kinetics Of Iron Ore With Coal

The mechanism of iron ore with coal is not fully understood [29] despite the numerous studies [30-39] that have been conducted on the subject. The complexity of reduction has rendered it difficult to gain a clear insight of the various steps that are involved in the overall reduction process. True direct reduction of iron ore is possible only when the gaseous product of the reaction, i.e. CO and CO_2 are removed from the reaction system as soon as they are generated. Stoichiometrically the process may be represented by equations (2.1) and (2.2)

$$Fe_xO_y(s) + C(s) = Fe_xO_{y-1}(s) + CO(g) \qquad (2.1)$$

$$2Fe_xO_y(s) + C(s) = 2Fe_xO_{y-1}(s) + CO_2(g) \qquad (2.2)$$

The reaction between two solid phases can only begin at points of contact between coal and iron ore. Contact is disrupted as soon as metallic iron appears as an intermediate phase. From then on, reduction can only proceed by the diffusion of carbon atoms through the metallic iron layer to metal oxide interface. The interfacial chemical reaction involving oxide and carbon is presumed to occur relatively fast as compare to diffusion process. It have been proposed [30, 31] that diffusion through the product layer i.e. reduced metallic layer, is the rate limiting factor in the direct reduction process.

Concerning the nature of reaction in a heated mixture of iron oxide and coal, several investigator have assumed the reaction to proceed according to following equations:

$$Fe_xO_y(s) + Y\ C(s) = X\ Fe(s) + Y\ CO(g) \quad (2.3)$$

$$Y\ CO(s) + Fe_xO_y(s) = X\ Fe(s) + Y\ CO_2(g) \quad (2.4)$$

$$Y\ CO_2(g) + Y\ C(s) = 2\ Y\ CO(g) \quad (2.5)$$

where Fe_xO_y stands for Fe_2O_3, Fe_3O_4 and FeO. Mechanism of all these reactions are reasonably well understood [15, 32-34]. It has generally been assumed that the overall rate is controlled by oxidation of carbon i.e. gasification reaction. Gasification of C by CO_2 is considerably slower than the reduction of iron oxide below 900°C. At higher temperature, however, the reaction rate is controlled by both the reactions (2.4) and (2.5).

Like reducibility of iron ore the reactivity of carbonaceous materials varies widely from one material to another and from batch to batch of the same material. The surface area of carbon available to provide reaction sites for the CO_2 is the an important feature and this is determined by the particle size and porosity. Processed materials such as charcoal, char and coke are more porous and reactive than natural carbon bearing materials such as coal, graphite and wood.

Ray and coworkers [35-37] have done extensive studies on reduction of iron ore fines with coal fines in a FBR in the temperature range 900-1000°C. Air has been used as a fluidizing medium. They concluded [36] that within the range of variables studied, an increase in reduction temperature and coal/ore ratio of the reduction mixture results in higher reduction rate,

whereas, an increase in air gas flow rate adversely affects the reduction rate. Apparent activation energy value for the reduction reaction is calculated to be 36.9 kcal/mol which is nearly half the value for true gasification of carbon by chemical reaction. Hence, they concluded that reduction was controlled by combination of carbon gasification and pore diffusion.

According to Szekely et al. [38], the iron oxide-carbon system is a complex one, therefore, there is neither a general rate equation nor a clear cut method for interpretation of kinetics data.

A number of investigators have performed the reduction of iron oxide with coal under different experimental conditions and have reported activation energy values .Some of these are compiled in Table 2.2.

Table 2.2 : Activation energy data for the reduction of iron ore with coal as a reducing agent

Material	Iron ore size(μm)	Coal size (μm)	Temperature (K)	Act..Energy (kcal/mole)	Reference
Iron Ore	1000-2000	1000-2000	1173-1323	37.86	Haque et al [36]
Iron Ore	180-250	353-500	1173-1273	36.19-37.62	Haque et al [37]
Iron Ore	250-500	250-500	1123-1323	40.09-42.07	Mookherjee et al [35]
Iron Ore	<150	150	1173-1373	25.75	Reddy et al [39]

2.1.3 Reduction Kinetics Of Iron Ore With Methane

Although a large number of investigations on reduction of iron oxide with gas mixtures consisting of H_2 and CO have been reported in literature in the recent past, very few studies can be found where hydrocarbon have been employed directly for reduction purposes. Nixon [40] has explained favourable result with butane injection by high reactivity of nascent CO, carbon and hydrogen produced by autocatalyzed reaction of hydrocarbon on the surface of partly reduced ore particles.

Ghosh et al. [41] performed a series of experiments involving reduction of iron oxide pellets by unreformed methane gas in the temperature range 800-950^{o}C using the gas flow rate between 45-170 cc/min. They explained their results assuming a two step mechanism. In the first step the methane is decomposed into carbon and hydrogen. The latter than reduces the oxide in the second step.

Hutchings et al. [42] performed a number of reduction experiments with H_2, H_2+CH_4 and CH_4. According to them the reaction of iron ore with H_2+CH_4 may be divided in to several stages. In the first, the reduction with the methane is undetectable since reduction by hydrogen is much faster and there is no metallic iron catalyst present initially for reforming methane [43]. It has been suggested that direct reduction with methane is much slower than that with the reformed gas. Ruprecht et al. [44] observed that after the reduction of hematite to magnetite, the magnetite to wustite step was slow. There was then

a marked increase in the rate as methane cracked on the freshly formed metallic iron. The inclusion of hydrogen in the reducing gas shortened the magnetite to wustite step and gave the better results. It was shown [42, 44] that during the reduction of iron ore with hydrogen and methane, the later was inert up to 30% reduction, corresponding to the conversion of bed to wustite. It was therefore, suggested that the methane may be used as a reducing gas in the final stages of reduction.

Table 2.3 :Activation energy data for the reduction of iron ore with methane as a reducing agent

Material	Size(μm)	Temperature(K)	Act.. Energy(kcal/mol)	Reference
Iron Ore	180-250	900-1100	50.0	Hutching et al[42]
FeO	-	973-1273	52.00	Barret et al [43]
Fe_2O_3	7600-12700	1073-1298	47.79-52.55	Ghosh et al [41]

2.2 Presence Of Carbon In Sponge Iron

Carbon in sponge iron may be present in the following forms.

a) As solid solution in the form of ferrite or austenite.

b) As cementite, Fe_3C, which is metastable in nature.

c) Free carbon as soot or char, mechanically entrapped in pores or on surface of sponge iron.

Carbon for sponge iron may be available from two sources.

1) Carbon deposited due to decomposition of CO present in the reducing gas

$$2\ CO \rightleftharpoons CO_2 + C \qquad (2.6)$$

Decomposition of C from CO is effective at low temperature i.e. below 900°C, while the gasification of carbon is preferred at higher temperature i.e. 1000°C.

2) Cracking of hydrocarbon present in the reducing gases.

$$C_xH_y \rightleftharpoons C + H + C_x.H_y. \qquad (2.7)$$

Carbon in sponge iron is of great operational and economic importance. It increases equivalent metallization of the sponge iron during melting. It combines with residual unreduced FeO to produce the metallic iron.

$$FeO + Fe_3C = 4\ Fe + CO \qquad (2.8)$$

The stoichiometric balance of the equation shows that 1.0% of carbon in sponge iron can reduce 5.35% of Fe if only CO is formed during the reaction.

Another favourable phenomenon that take place in Electric Arc Furnace (EAF) due to presence of carbon in sponge iron is formation of CO gas which offers following beneficial consequences.

i) The slag-metal interface area is increased and the impurity refining rate is greatly enhanced with the rapid agitation.
ii) The low slag density permits rapid penetration of sponge iron to the slag-metal interface, thus solving the problem of "iceberg formation" in steel bath.

However, such an amount of carbon can not be easily made up by additional charging of 'say' broken electrode during melting in EAF since recovery of carbon in later case is less than 20% while combined carbon is almost fully utilized.

2.3 Commercial Sponge Iron Making Processes Based On FBR

At present there are only two commercial processes, which use FBR, are under operation in Venezuela, namely HIB and FIOR processes.

2.3.1 HIB (High Iron Briquette) Process

In this commercial reduction process [45, 46], being commercially operated at Puerto order, Venezuela, fine iron ore is reduced in a two stage FBR. Reduction of Fe_2O_3 to FeO is accomplished in the first stage by the contact with flue gases from the second (lower) stage. Reduction of FeO to Fe is

accomplished in second stage by contact with fresh reducing gas. Reformed natural gas is used here as reducing agent. reduced fine are compacted and then sent to the briquetting rolls. The product of this process has a metallization of 62-65 percent and carbon content 0.19% only which is considered quite low for its end use for steel making, especially in EAF.

2.3.2 FIOR (Fluidized Iron Ore Reduction) Process

This process is also under commercial operation at Puerto Ordaz, Venezuela [45, 46]. The reduction of iron ore fines basically take place in four FBRs including ore preheater reactor. The iron ore flows downward through the FBR by gravity and the flowing ore is maintained in the fluidized state, while at the same time reduced by the circulating reducing gas. Reducing gas is the reformed natural gas, reformed into CO and H_2 by means of steam and catalysts. Here also briquetting is done in hot condition. The FIOR briquettes are of high metallization in the range 92-94% and carbon content is nearly 2%.

CHAPTER 3

SCOPE OF THE PRESENT INVESTIGATION

The two industrially viable FBR based processes in South America, as discussed in chapter 2, use reformed natural gas as the reducing agent. Since substantially high flow rate of reducing gas is generally required to fluidize the solid particles in FBR, these process are not likely to be economically viable in our country where natural gas is comparatively more expensive. Present investigation aims at an alternative direct reduction process producing sponge iron by reduction of iron ore with coal fines and natural gas together as reducing agents.

The present investigation has been divided into four parts.

i) In the first part of our investigation, a number of experiments have been carried out with hydrogen as a reducing agent. These experiments are essentially used as the reference for the subsequent reduction experiments. It was decided to see the effect of temperature and reduction time on the reduction of iron ore with hydrogen in a FBR. In all about 13 experiments have been carried out in this part by varying temperature between 900-1000^{o}C and reduction time in the range 15-120 minutes. Hydrogen and argon gas mixture has been used in all these experiments.

ii) The second part of this investigation essentially deals reduction of iron ore with solid carbonaceous reducing agent

(coal) using argon as a fluidizing medium. In all about 18 experiments have been performed in this part using three different types of coals. These experiments are expected to show the effect of coal reactivity on the overall reduction process. In these experiments temperature has been varied between 900-1000^{o}C and the reduction time ranged between 15-120 minutes. Final product, which consists of a mixture of coal, unreduced iron ore and sponge iron is first subjected to sieving and then magnetic separation to separate coal and sponge iron from the unreduced ore.

iii) The role of methane as a reducing agent has been investigated in the third part of this study. In all experiments with methane, argon is used as a fluidizing medium. During the course of these experiments, the initial rate of reduction was found to be unexpectedly very sluggish. To examine whether or not the initial metallic iron acts as a catalyst for subsequent reduction with methane, this part of an experimental plan was somewhat modified during the course of investigation. A few additional experiments were planned in which the initial reduction was carried out with hydrogen and then methane hydrogen mixture was used as the reducing agent.

iv) A sponge iron making process based on reduction of iron ore with hydrogen and methane mixture is not likely to be economically viable in our country where both the gases are expensive. Also such a process will defeat the basic objective of utilizing large amount of coal fines available in our country. It has, therefore, been speculated that an optimal process would be the one in which

iron ore is partially reduced with coal and partially with methane. To examine the feasibility of such a process about 12 experiments were carried out in which coal and methane were used as reducing agents simultaneously. In these experiments the reduction time was varied between 15-60 minutes while the temperature ranged between 900-1000^{o}C. After each experiment coal and sponge iron were separated from the unreduced ore by sieving and magnetic separation, respectively

To estimate the extent of reduction and to determine the degree of metallization the final product of each experiment has been chemically analyzed to estimate the total iron and the metallic iron present in the sponge iron. A few samples have also been subjected to X-ray diffraction analysis to identify the phases present.

CHAPTER 4

EXPERIMENTAL

This chapter deals with the design of the fluidized bed reactor, experimental set up, selection of different materials, and experimental procedure for different reducing agents. This is followed by the characterization of the reactor product by chemical analysis and X-ray diffraction.

4.1 FLUIDISED BED REACTOR (FBR) ASSEMBLY

Based on the results of the cold model FBR study, the high temperature FBR was designed and fabricated by Kumar [47]. The same reactor has been used in this study. The schematic representation of this assembly is shown in Fig.4.1. It consists of a FBR and preheater. A brief description of these is given below.

4.1.1 Fluidized Bed Reactor (FBR) Design

The theoretical aspects of FBR design are discussed briefly in Appendix A. The dimensions of the main reactor are exactly the same as that of the cold model FBR [47]. The reactor chamber is made of 5.2 cm diameter and 60 cm long stainless steel (SS) tube with a thickness of 3.0 mm. The distributor plate is sand-wiched at the bottom end of the reactor and another 10.0 cm long tube of same diameter and thickness. All the three (bottom end of reactor tube, distribute plate and another 10 cm long tube) are fitted tightly with the help of nuts and bolts. The 10 cm long tube is

completely filled up with the 0.5 inch diameter mild steel balls to ensure proper distribution of fluidizing gas. The FBR is connected to the preheater tube through a 1.0 cm diameter and 25.0 cm long SS tube. This tube is adequately insulated to minimize the heat losses. A SS head covers the top end of the reactor tube which is outside the furnace. Three openings are drilled through this head. A SS tube welded to the head through an opening at its centre provides an outlet for the reactor flue gases. This SS tube is brazed to 150.0 cm long and 1.5 cm diameter copper tube with an aim to cool the exit gases to the room temperature. Through one of the other openings, a chromel-alumel thermocouple is introduced in the reactor in such a way that its tip is just 1.0 cm above the distributor plate. This arrangement ensures that the tip of the thermocouple always remains dipped inside the bed and records bed temperature during the reduction experiments. The third opening on the SS head is for feeding solid powder to the reactor chamber. This hole can be sealed with a tightly fitting bolt immediately after the sample is introduced into the reactor chamber.

4.1.2 Preheater Design

As the reduction of hematite with coal, hydrogen and/or methane is endothermic it is essential to preheat the fluidizing and the reducing gases to the reactor temperature. In order to heat the gases from room temperature to a temperature as high as 800-900^{o}C a sufficiently long preheater is required. Since a FBR is generally operated at 5-20 times the minimum fluidization velocity [49], the residence time of gas in the preheater is short. Because of non-availability of long enough furnace muffle

which can contain both the reactor and the preheater, the preheater is seperated from the reactor.

The preheater is made of 70.0 cm long and 5.2 cm diameter SS tube which can be independently heated. The preheater tube is completely filled up with 0.5 inch diameter mild steel balls to enhance the heat transfer from the preheater to the gas flowing through it because of high heat content of these balls. These balls also result in increased residence time of the flowing gas because of tortuous path that the gas has to take. Both the top and the bottom ends of the preheater are connected to SS heads. Through the top head the preheater is connected to the main reactor, whereas the bottom head is connected to the gas line providing the fluidizing and/or reducing gas to be preheated.

All joints in the reactor and the preheater assembly are provided with gaskets made of high temperature material and these are sealed with high temperature sealant to make the reactor leak-proof.

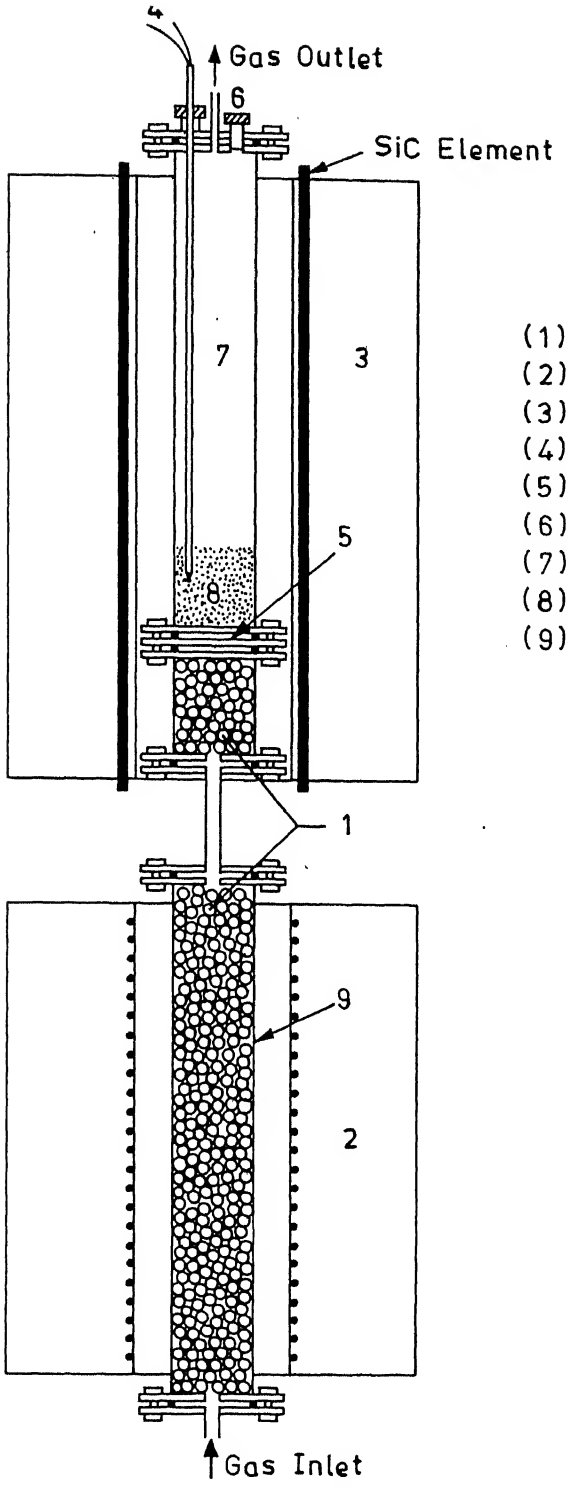

(1) Mild Steel Balls
(2) Kanthal Wire Wound Furnace
(3) SiC Heating Element Furnace
(4) Thermocouple
(5) Distributor Plate
(6) Feeding Port
(7) Reactor
(8) Soid Particles
(9) Preheater

Figure 4.1 : High temperature fluidized bed reactor assembly details

4.2 EXPERIMENTAL SET UP

Two furnaces have been designed to heat the FBR and the preheater independently. In both the furnaces, tubes are alumina tubes of 7.6 cm diameter and 60.0 cm length. The preheater furnace is kanthel wire wound furnace with total resistance of 40 ohms and a power output of 1.25 kw. This is designed to produce a preheating temperature of 800-900^{o}C. The reactor furnace uses six silicon carbide rods as the heating elements. Each rod has 1 ohm resistance. The power output of this furnace is almost twice that of the preheater furnace. A temperature as high as 1150^{o}C can be achieved in this furnace. The FBR and the preheater furnaces are arranged one above the other, reactor furnace occupying the top position, such that their axes are aligned. The two furnaces are separated by a distance of around 25.0 cm.

A gas train shown in Fig.4.2 is used to remove moisture and oxygen from the inlet gases. It consists of series of calcium chloride and pyrogallol columns and a copper gauze furnace. Calcium chloride columns are used to remove moisture. Copper gauze furnace and pyrogallal columns are used to remove oxygen impurities from the fluidizing gas before it entered the preheater. A rotameter and a calibrated capillary flow meter are provided to measure flow rates of inlet gases.

The FBR and the preheater assembly are introduced into the respective furnaces such that the reaction zone in the reactor exactly coincides with the constant temperature zone of the reactor furnace. To achieve a good temperature control in FBR an

indicator control system has been istalled. This can provide a temperature control within $\pm 5^{o}C$. The temperature of preheater furnace, however, is controlled manually by changing voltage of the supply. A temperature control of $\pm 10^{o}C$ is achieved in this case.

The outlet of the FBR is connected to a water trap with the help of a rubber tube. Entrained solid particle are removed here. The gas from water trap is passed through a series of calcium chloride columns before connecting it to a capillary flow meter to measure the exit flow rate of flue gases.

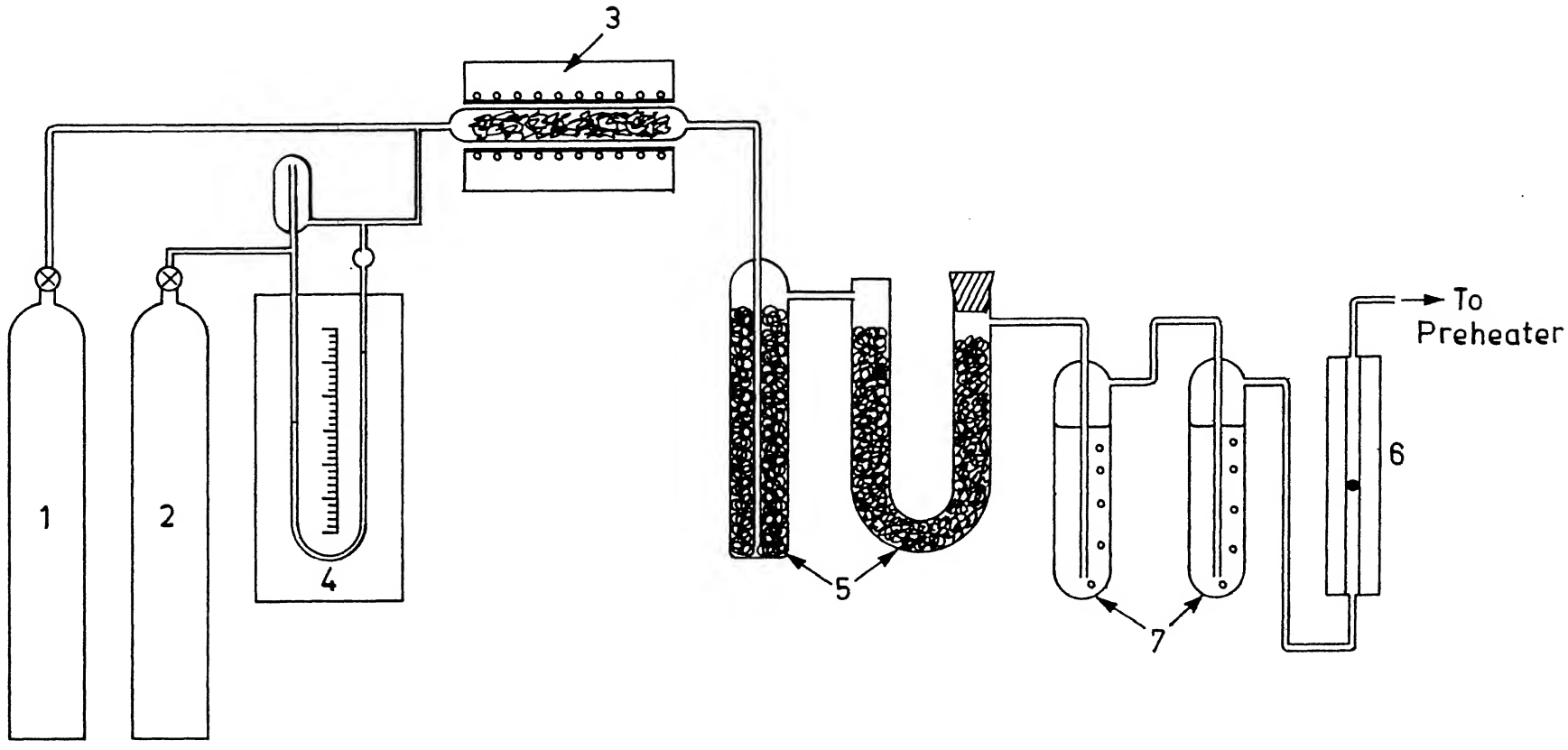

(1,2) Gas Cylinders (3) Copper Gauge Furnace (4) Capillary Flow Meter
(5) Anhydrous Calcium Chloride (6) Rotameter (7) Pyrogallol Bubbler

4.3 MATERIALS

4.3.1 Iron ore

Iron ore used in present investigation is of Barsua mines consisting 64.96 % total iron. 70 g of iron ore in the size range -100 +150 mesh was used in the each experiment.

4.3.2 Coal

Several types of coal fines in the size range -35 +60 mesh are used in the present investigation. The coal fines are deliberately chosen coarser then the iron ore fines to avoid elutriation of coal fines during the fluidized state. Proximate analysis of these coals is given in Table 4.1.

Table 4.1 : Proximate analysis of different coals used in the present investigation.

source	fixed carbon	volatile matter	ash content
Bhurkunda mine	35.50 %	29.95 %	34.55 %
Samla mine	45.97 %	32.28 %	21.75 %
Wood Coal	75.3 %	23.7 %	1.0 %

4.3.3 Gases

Hydrogen and Argon gas cylinders (IOL Delhi) with a purity of 99.9% are used in the present investigation. It is further purified in the lab using gas train shown in Fig. 4.2. Since the

methane gas was not readily available in the local market at an affordable price, it was decided to generate and store the methane gas in laboratory itself.

4.3.3 a) METHANE GENERATION SET UP AND STORAGE ASSEMBLY

Fig.4.3 shows the schematic diagram of the set up for generation and storage of the gas. The gas is produced by carrying out a reaction between anhydrous sodium acetate and sodalime.

$$CH_3COONa + NaOH = Na_2CO_3 + CH_4 \qquad (4.1)$$

It is usually recommended to take sodium hydroxide in the form of sodalime. Sodalime is prepared by grinding and intimately mixing sodium hydroxide pellets with calcium oxide in the ratio 7:3. The resulting sodalime and anhydrous sodium acetate are taken in 5:4 ratio, ground and mix thoroughly. After several trials, It could be established that the optimum temperature for methane generation was 400^{o}C. As it is not possible to supply the methane generated according to the reaction (4.1) directly to the reactor at a controlled flow rate, storage and pressurization of the gas is necessary.

A mixture of 75 gms anhydrous sodium acetate and 60 gms of sodalime is introduced in to pyrex tube which is gradually inserted into the furnace maintained at 400^{o}C. However, before doing so, the storage vessel made of stainless steel is kept completely filled up with water up to the level of valves V_5 and V_1, valve V_4 is closed. By opening the valve V_3 water is allowed

to enter the gas storage tank (5) from the overhead tank (7). In this way the air inside the gas storage tank (5) is expelled out by opening the valves V_1 and V_2. After this, valves V_3, V_4, V_5 and V_1 are closed. Towards the start, the valve V_5 is kept closed as lot of air comes out along with methane. This impure methane is vented out through a bypass (valve V_6). After some time, when gas generation rate becomes appreciable (which is indicated by the exit gas through the bubbler 3), valve V_5 is opened. To displace water from the gas storage tank to provide space for gas storage, valve V_4 is also slowly opened up. While the valve V_2 is kept closed but the valve V_1 remains open to record the pressure of the gas accumulated in the gas storage tank, with the help of a manometer. After the completion of methane generation, the valves V_5 and V_4 are closed and the valve V_3 is opened to allow the entry of water into the gas storage tank (5) from the over head tank (7). This way gas is compressed to a certain extent and is ready for use.

During the use of methane for reduction, the pressure of the gas in storage vessel tends to drop. It is maintained almost constant because of inflow of water from overhead tank (7) in the gas storage vessel (5). The water head in the overhead tank (7) is maintained constant by ensuring overflow to drain all the time. Pressurized methane gas attains approximately a pressure of 1.2 atmosphere.

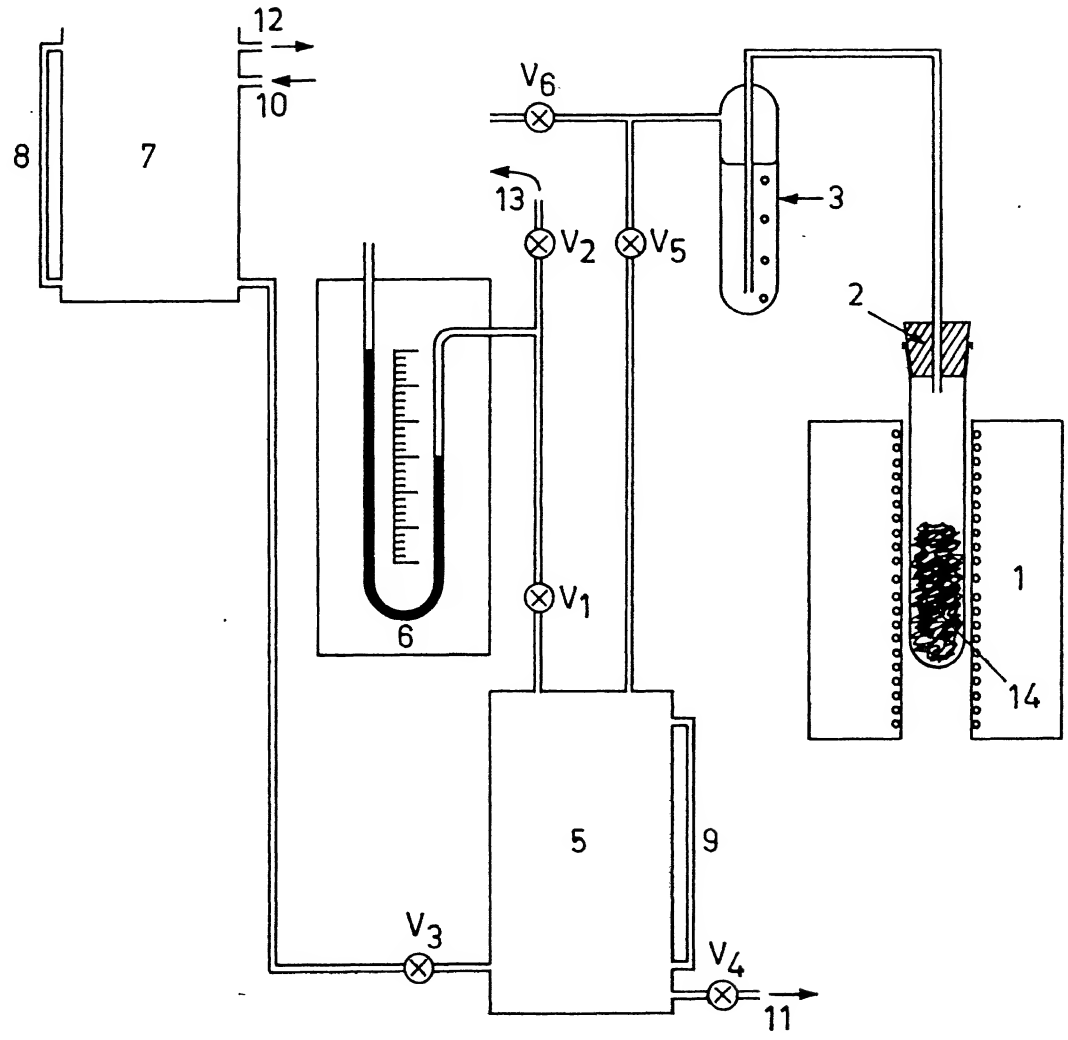

(1) Kanthal Wire Wound Furnace
(2) Neoprene Stopper
(3) Bubbler
(4) Valves (V_1,V_2,V_3,V_4,V_5 & V_6)
(5) Methane Gas Vessel
(6) Mercury Manometer
(7) Pressurising Water Tank
(8,9) Water Lavel Indicator
(10) Water Inlet
(11) Water Outlet
(12) Overflow to Drain
(13) Methane Gas Outlet
(14) Sodalime and Sodium Acetate.

4.3.4 Sealents and Cements

High temperature sealents and cements are used to make reactor leak proof.

Silicon Sealent (SILASTIC 732 RTV) Dow coring corpn., USA

Alumina Cement Dow coring corporation, USA

4.3.5 Chemical Reagents

A number of chemical reagents are used in chemical analysis and methane generation. These are listed below.

Anhydrous Sodium Acetate (GR) (Sarabhai M Chemicals, Bombay)

Sodium Hydroxide (LR) (Ranbaxy Laboratories Limited, Punjab)

Potassium Hydroxide (LR) (Ranbaxy Laboratories Ltd, Punjab)

Calcium Oxide (LR) (LOBA Chemic Pvt Ltd, Bombay)

Sulfuric Acid (AR) (Indian Drug and Pharm Ltd, Hydrabad)

Hydrochloric Acid (AR) (Arc Industries, Kanpur)

Stannus Chloride (AR) (LOBA Chemic Pvt Ltd, Bombay)

Calcium Chloride (LR) (Ranbaxy Laboratories Pvt Ltd, Punjab)

Potassium Dichromate (AR) (Ranbaxy Lab. Pvt Ltd, punjab)

Mercuric Chloride (LR) (E. Merck (India) Ltd, Bombay)

Phosphoric Acid (LR) (Wilson Chemicals, Bombay)

Sodium Diphenylamine Sulfonate (GR) (LOBA Chemic, Bombay)

4.4 EXPERIMENTAL PROCEDURE

Experimental procedure can be divided into two parts, namely, reduction experiments and characterization of reactor product.

4.4.1 Reduction Experiments

To start the reduction experiment, the three furnaces, namely, the reactor, the preheater and the copper gauze furnaces are switched on and set to the pre-specified voltages. Sufficient time is allowed for attainment and stabilization of the set temperatures. It takes around 7-8 hours to attain a temperature of 950^{o}C. First the reactor is flushed with argon for about 15.0 minutes and after that a dried and weighed feed is introduced through the top hole of the reactor with the help of a long metallic funnel. This top hole is immediately closed with the help of a tightly fitting bolt after introducing the feed into the reactor. The quantity of feed material is chosen such that the height of the static bed is about one inch. The temperature of the reactor furnace generally decreases by 150-300^{o}C on feeding the cold charge. Therefore, before starting the fluidization of the bed the temperature of the reactor furnace is restored maintaining a low flow rate of argon just sufficient to flush any air that might have entered the reactor with the solid charge and also to avoid any further diffusion of atmospheric air into the reactor. It takes about 5-24 minutes to restore the reactor temperature. From the cold model studies for the particle sizes involved in the present investigation, the minimum fluidization velocity was estimated to be around 0.76-1.60 cm/sec. To ensure complete fluidization, all the experiments have been carried out at a total gas flow rate (STP) of 5.0 liter per minute. The fluidizing and reducing gases are introduced in to the reactor for a specified time and at a total gas flow rate of 5 liter per minute after the reactor temperature is attained and stabilized at the prespecified

temperature. A number of reducing agents are used in present investigation.

At the end of an experiment, the flow of argon is reduced to a very low level and the flow of the reducing gas is stopped. The reactor and the preheater furnaces are switched off. The copper gauze furnace remains switched on to remove oxygen from argon. Argon is continued to flush the reactor till the reactor furnace is cooled to a temperature of 300^{o}C to avoid reoxidation of the FBR product due to the air entrainment. After the reactor assembly is cooled down to room temperature, the FBR product is taken out. The sponge iron thus obtained is chemically analyzed to estimate the metallic iron and the total iron present. To identify phases present in the FBR product, sponge iron samples have also been analyzed using X-ray diffraction.

4.4.1 a) Reduction with Hydrogen

A number of studies have been reported in literature related to the hydrogen reduction of iron ore. Since iron ore reduction is dependent upon iron ore characteristics and process design, it was decided to study reduction behaviour of our iron ore in hydrogen. Details of these experiments are given in Table 5.1. In this series of experiments hydrogen-argon mixture served both as the fluidizing medium as well as the reducing gas.

4.4.1 b) Reduction with Coal

In this series of experiments, coal is used as reducing agent while argon is the fluidizing gas. Different types of coals have

been used for reduction purposes. Proximate analyses of these coals are given in Table 4.1. In these experiments weight of coal is chosen such that the fixed carbon is 50 % extra than that stoichiometrically required for complete reduction. Details of these experiments are given in Table 5.2.

4.4.1 c) Reduction with Methane and Hydrogen

In a few experiments methane-argon mixture has been used as the fluidizing as well as the reducing gas. As only negligible amount of metallic iron was observed in these experiments, in the next series of experiments hydrogen and methane mixture is used as a reducing agent. As hydrogen starts the reduction, the metallic iron thus produced acts as a catalyst for methane reforming. Details of these experiments are given in Table 5.3.

4.4.1 d) Reduction with Coal and Methane

In this series of experiments, coal and methane served as reducing agent. In these experiments methane is also acting as the fluidizing gas. weight of coal is chosen such that fixed carbon is stoichiometrically required for complete reduction. Details of these experiments are given in Table 5.4.

4.5 CHARACTERIZATION OF FBR PRODUCT

Final product of FBR is chemically analysed to determine the metallic and total iron. Few samples are also analyzed with the help of X-ray diffractgraph analysis.

4.5.1. Determination of total iron in the sponge iron

0.5 g of sponge iron is taken in a conical flask and 25 cc of conc. Hcl is added. It is then heated on a hot plate slowly till the solution becomes yellow in color and no black particles are visible in the solution. It is diluted to 250 ml in a volumetric flask. 50 ml of this solution is taken in to a conical flask and heated to boiling. Stannous chloride solution is added drop wise till the solution become colourless and one or two drops are added in excess. This solution is cooled to room temperature. 10 ml of 15% mercuric chloride is added in this solution and it is left for 10 minutes. Silky precipitate, white in colour is formed. 20 ml of acid mixture and 5 drops of diphenylamine indicator solution are added. This solution is titrated against standard N/10 $K_2Cr_2O_7$ solution and the amount of total iron in the sponge iron is calculated. This is repeated twice to check the result.

1 ml of N/10 $K_2Cr_2O_7$ = 0.0056 gm Fe

To make stannous chloride solution, 30 g of $Sncl_2$ is added in 100 ml conc. Hcl. It is diluted to 200 ml in a volumetric flask.

Mercuric chloride solution is made by adding 986 ml of distill water in 64 g of $Hgcl_2$. It is diluted to 1000 ml in a volumetric flask.

Acid mixture is made by adding 150 ml of conc H_2SO_4, 150 ml of phosphoric acid and 700 mm of distill water.

Diphenylamine indicator is made by adding 100 ml of sulfuric acid to 1.0 g of sodium diphenylamine sulfonate.

N/10 $K_2Cr_2O_7$ solution is made by adding 1000 ml of distill water in 4.903 g of $K_2Cr_2O_7$ in a volumetric flask.

4.5.2. Determination of metallic iron in the sponge iron

100 ml of distilled water is taken in a conical flask and heated to boiling. 1.0 g of sponge iron and 3.0 g of mercuric chloride are added to conical flask. Solution is heated for 15 minutes and then allowed to cool down to room temperature. It is filtered and diluted to 100 ml in volumetric flask. 25 ml of this solution is taken in a conical flask. 10 ml of 25 % sulfuric acid and 3.0 ml of phosphoric acid are added to this solution. 5 drops of diphenylamine indicator solution is also added to this solution. This solution is titrated against N/10 $K_2Cr_2O_7$ and amount of metallic iron in sponge iron is calculated. Titration is repeated twice to check the result.

1 ml Of N/10 $K_2Cr_2O_7$ =0.0056 g of Fe

4.5.3 X-ray Analysis of FBR Product

The X-ray analysis of FBR products is carried to identify the phases present. Copper (K_α) target is used for this purpose with Ni filter. The other conditions are

Scanning speed = 3°/min in 2θ

Chart speed = 3 cm/min

Counts/sec = 1 K

Time constant = 3 sec

20 mA/30 KV

CHAPTER 5

RESULTS AND DISCUSSION

As mentioned in the previous chapter, four set of experiments were performed by varying reaction temperature, reduction time and the reducing agent itself. Hydrogen was used as a reducing agent in the first set of experiments while in the second set a solid carbonaceous material, such as coal, was used as a reductant. In the third set methane-hydrogen mixture was used as a reducing agent. In the last set of experiment the reduction was carried out using coal and methane as reducing agents simultaneously.

For each experiment the extent of reduction and degree of metallization were determined using the procedure suggested by Gonzales and jeffes [48]. Using percent reduction versus time data at various temperatures, activation energy for the reduction of iron ore was calculated and compared with the already reported values in the literature.

A few experiments were also repeated to check the reproducibility of the experimental data, and results are found to vary within a range of ±10% . For a complicated system like a fluidized bed reactor operating at high temperature, this much variation is well within the acceptable limits. In this chapter the results of various experiments are presented and discussed.

5.1 Reduction of Iron Ore With Hydrogen

In this series of experiments of iron ore samples were reduced at three different temperatures: 900, 950 and 1000°C using a gas mixture of hydrogen (2.0 l/min) and argon (3.0 l/min). Reduction time was varied between 15-120 minutes. After an experiment was over, the final product was chemically analyzed to determine metallic iron and total iron. Both (total iron and metallic iron) are plotted as a function of time at three temperatures in Fig.5.1. The extent of reduction was determined with the help of total iron in the reduced sample using a method suggested by Gonzales and Jeffes [48]. Detailed derivation of this method is presented in APPENDIX B. According to this method the extent of reduction can be written as

$$\% R = \frac{112}{48}\left[\frac{\%Fe_t^r - \%Fe_t^i}{\%Fe_t^r\ \%Fe_t^i}\right]\times 10000 \qquad (5.1)$$

where R is the percent reduction, Fe_t^r is the percent total iron in the reduced sample and Fe_t^i is the percent total iron in the initial sample. Extent of reduction was calculated using Eq. (5.1) and plotted as a function of time at three temperatures in Fig.5.2. From percent reduction, extent of metallization was calculated using the equations given below [48]

$$M(R\leq 40\%) = 0.25 - 5.65\times 10^{-3}R^2 + 3.94\times 10^{-4}R^3 \qquad (5.2)$$

$$M(R\geq 40\%) = -9.81 + 1.972\times 10^{-2}R^2 - 8.74\times 10^{-5}R^3 \qquad (5.3)$$

where M is the percent metallization and R is the percent

reduction. The above equations are based on regression analysis of extensive plant data from fixed beds, FBRs with a wide range of particle size, reducing gas composition, temperature, etc [48]. Percent metallization values obtained from Eqs (5.2) and (5.3) were compared with these computed from experimentally obtained metallic iron and total iron values as reported in Table 5.1. The agreement was quite good -within ±10%. Experimentally obtained metallization values are plotted as a function of time in Fig.5.3.

It is assumed that the overall reduction is controlled by a first order rate process, the rate of reaction may be given by

$$\frac{dW(t)}{dt} = -k\, W(t) \qquad (5.4)$$

where W(t) is the mass of reactant at time t and k is the reaction rate constant. In the integrated form this equation can be rewritten as

$$\ln\left[\frac{W(t)}{W(o)}\right] = -k\, t \qquad (5.5)$$

or

$$\ln(1-\alpha) = -k\, t \qquad (5.6)$$

where W(o) is the initial mass of the reactant and α is the fraction reduction. Thus, from Eq.(5.6), a plot of $-\ln(1-\alpha)$ vs time should be a straight line with a slope equal to k. Using the percent reduction data, plots of $-\ln(1-\alpha)$ vs t were obtained at three different temperatures, as shown in Fig.5.4.

It may be noted that the plots are linear in the initial stages of reduction but exhibit a non-linear behaviour in the later stages. This change in behaviour may be attributed to change in reduction mechanism i.e. the rate controlling step. It is quite likely that in the initial stages the overall rate of reaction is controlled by the rate of chemical reaction while after some time diffusion takes over as the rate controlling step.

Assuming Arrhenius law to be valid

$$k = k_o \exp\left(-\frac{E}{R\,T}\right) \qquad (5.7)$$

where k_o is a frequency factor, E is the activation energy and R is the universal gas constant. Plot of $\ln(k)$ vs $\frac{1}{T}$ was obtained as shown in the Fig.5.5. The activation energy calculated from the slope of the straight line is 14.85 kcal/mol. This value falls within the range of 10.87-19 Kcal/mol, as reported in literature (Table 2.1).

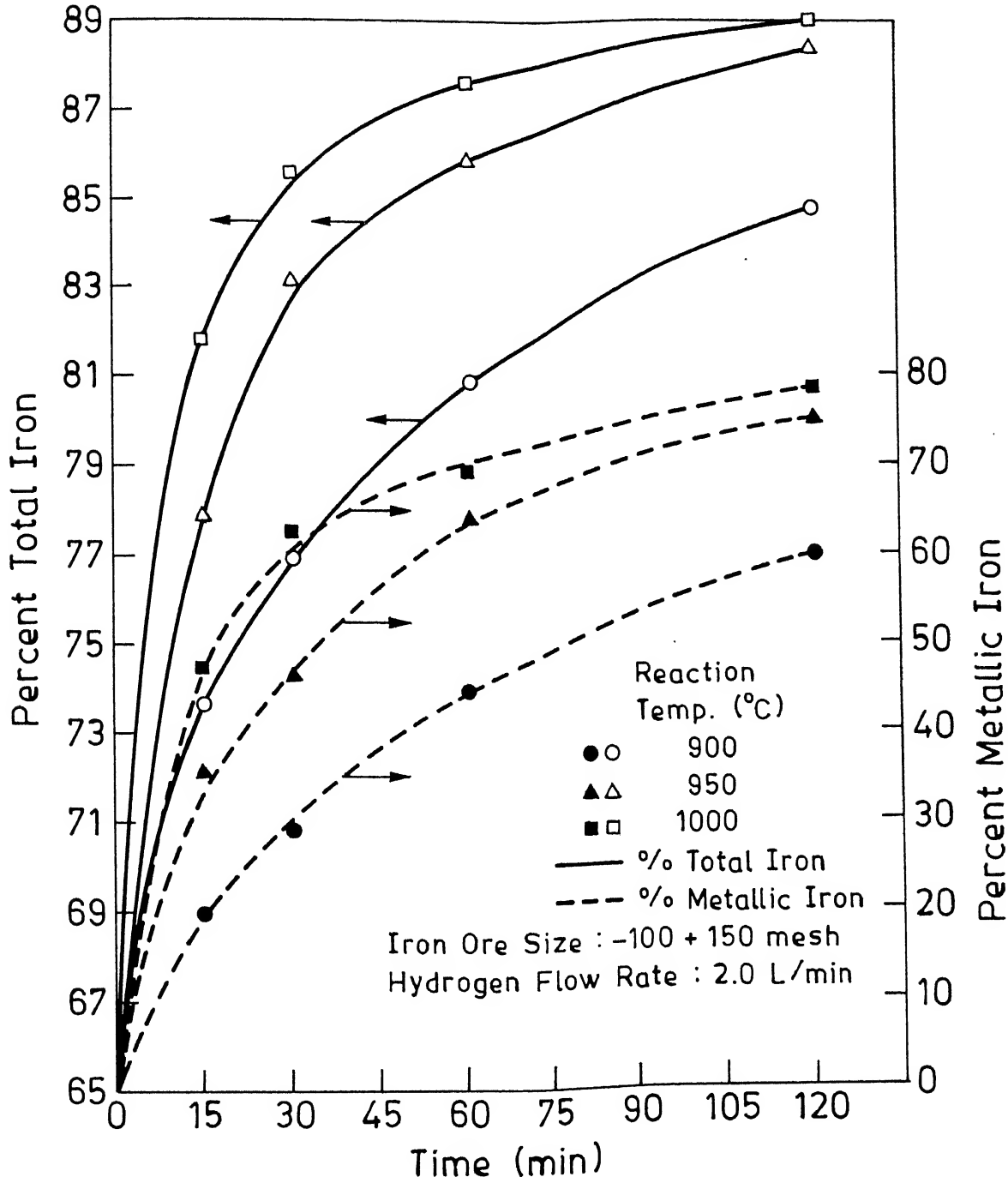

Figure 5.1 : Plot of percent total iron and percent metallic iron in the reduced sample as a function of time at three different temperatures in the case of reduction with hydrogen.

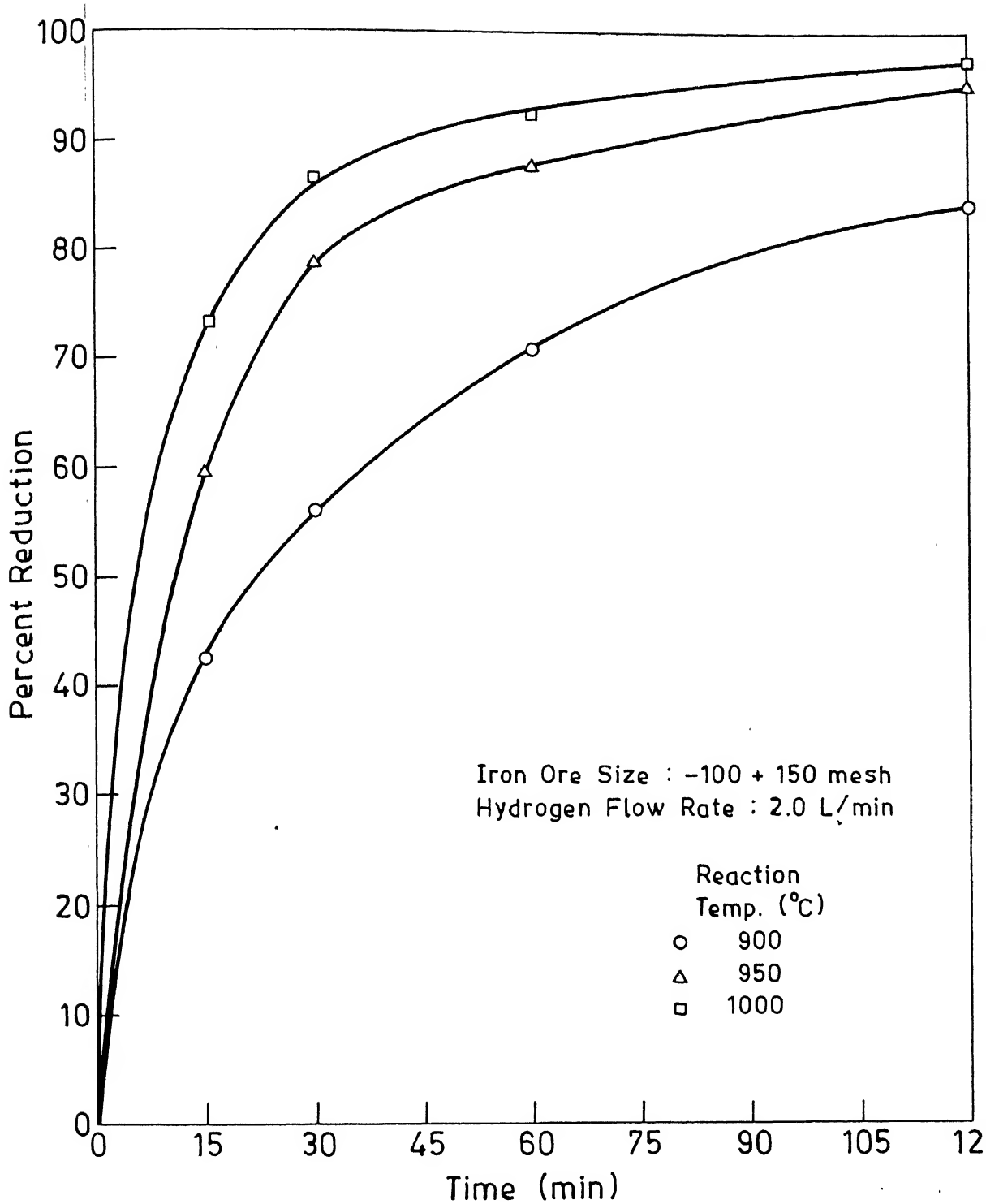

Figure 5.2 Plot of percent reduction as a function of time at three temperatures in case of reduction with hydrogen.

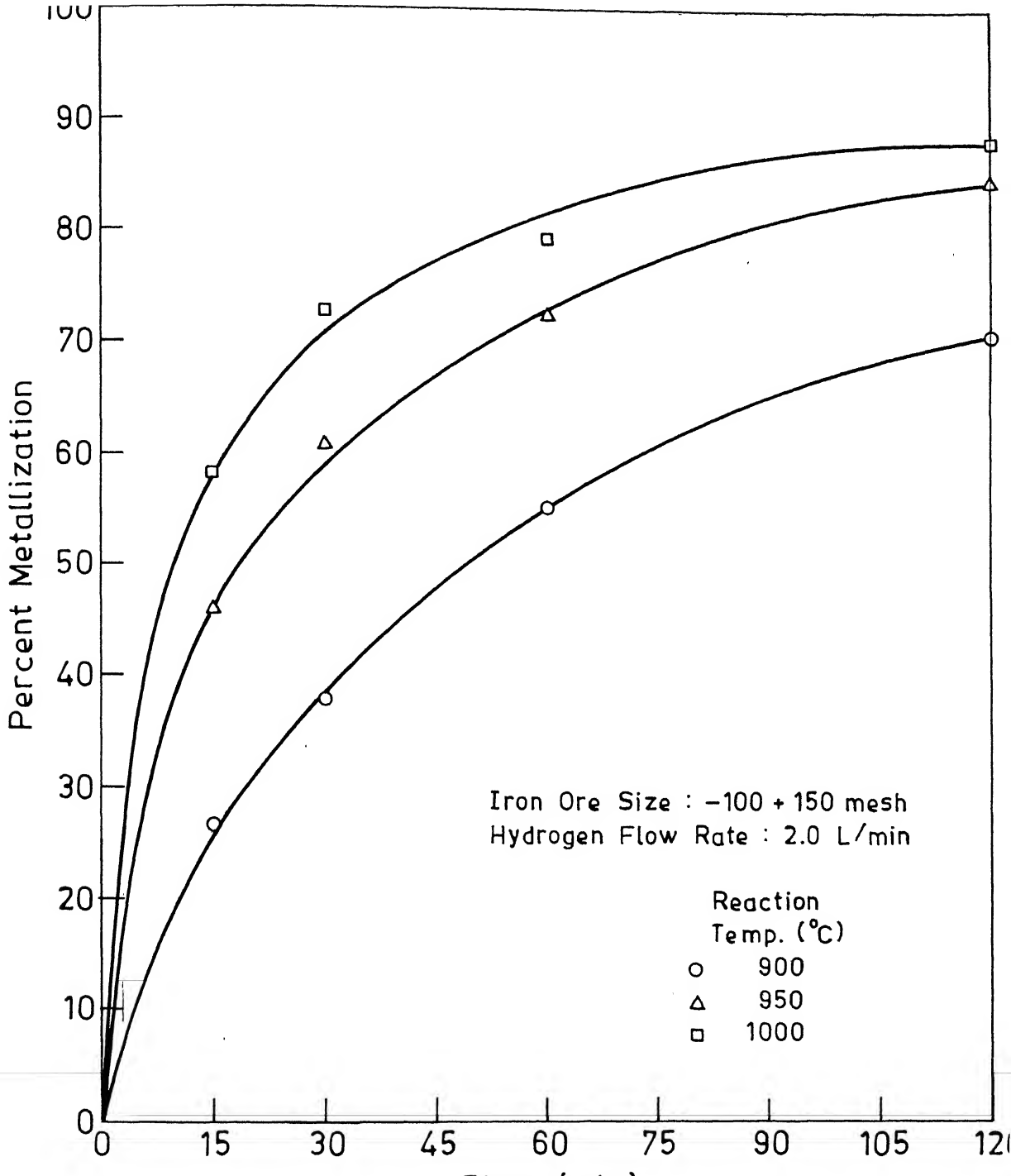

Figure 5.3 Plot of percent metallization as a function of time at three temperatures in case of reduction with hydrogen.

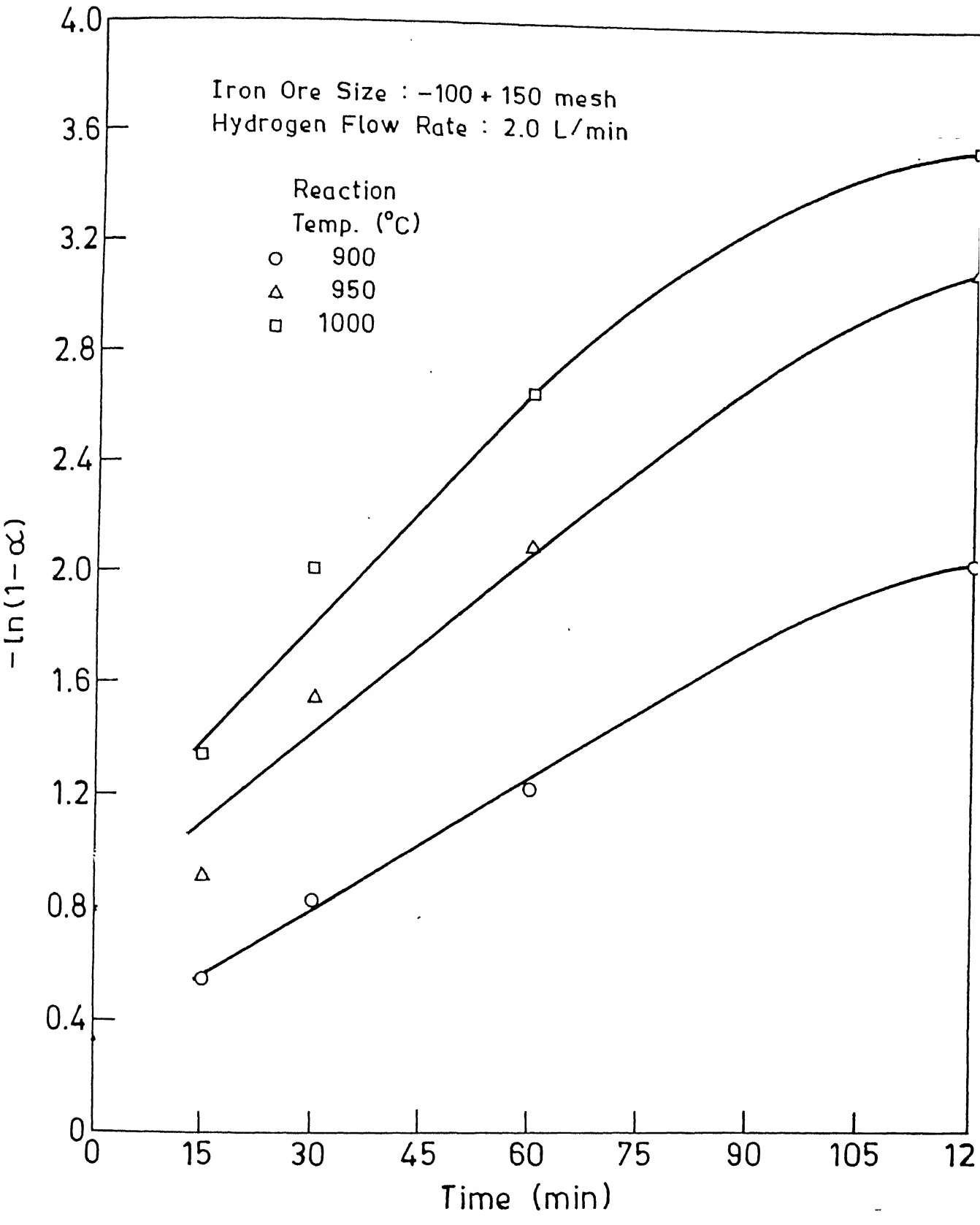

Figure 5.4: Plot of $-\ln(1-\alpha)$ as a function of time at three temperatures in case of reduction with hydrogen.

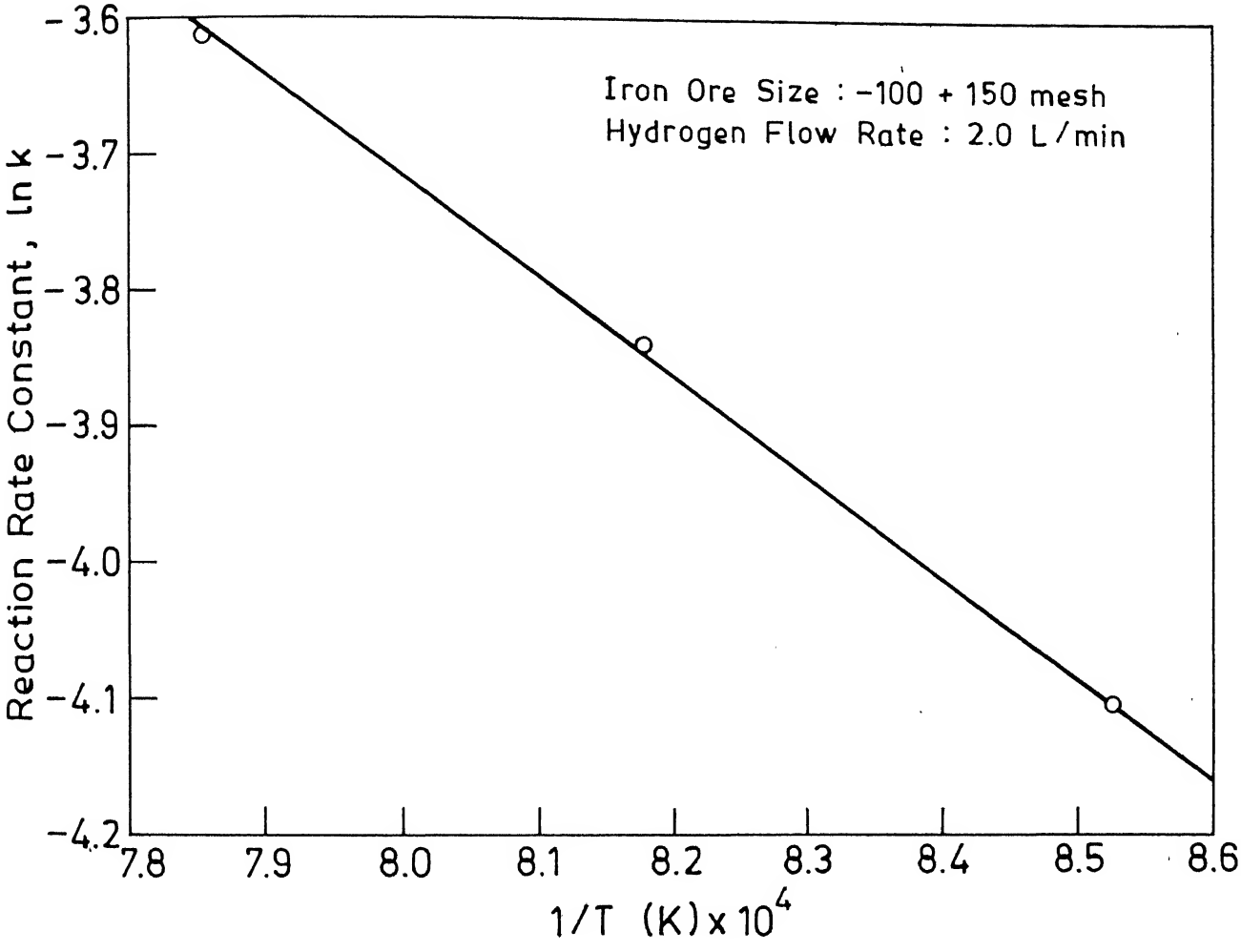

Figure 5.5: Plot of ln(k) as a function of reciprocal of temperature in case of reduction with hydrogen.

Table 5.1 : Different experimental condition and obtained result of iron ore reduction with hydrogen as a reducing agent

	t (min)	T (^{o}C)	$\%Fe_m$	$\%Fe_t$	%R	$\%M_{ex}$	$\%M_{th}$
EH1	15	900	20.2	73.64	42.66	27.43	20.56
EH2	30	900	29.0	77.00	56.17	37.66	36.90
EH3	60	900	45.0	80.92	70.84	55.61	58.08
EH4	120	900	60.0	84.84	84.167	70.72	77.78
EH5	15	950	35.84	77.84	59.44	46.04	42.40
EH6	30	950	51.3	83.14	78.54	61.70	69.48
EH7	60	950	64.4	85.96	87.75	74.92	82.98
EH8	120	950	75.0	88.48	95.49	84.765	93.90
EH9	15	1000	47.8	81.76	73.80	58.464	62.46
EH10	30	1000	63.0	85.68	86.86	73.53	81.69
EH11	60	1000	69.5	87.64	92.95	79.30	90.37
EH12	120	1000	78.5	89.04	97.14	88.163	96.15
EH6#	30	950	52.69	83.44	79.55	63.14	70.18

t is the reduction time in minutes

T is the reduction temperature in ^{o}C

$\%Fe_m$ is the percent of metallic iron in the reduced sample

$\%Fe_t$ is the percent of tatal iron in the reduced sample

%R is the percent reduction in the iron ore after the experiment

$\%M_{ex}$ is the % metallization based on the experimental results

$\%M_{th}$ is the % metallization based on the Eqs 5.2 and 5.3

is the experiment repeated to check the reproducibility

CENTRAL LIBRARY
I I T. KANPUR

5.2 Reduction of Iron Ore With Coal

In this set, experiments on reduction of iron ore (-100 +150 mesh) were carried out at three different temperatures, namely, 900, 950 and 1000^{o}C using coal (-35 +60 mesh) as a reducing agent. Argon is used as a fluidizing medium. As mentioned above also coal size was deliberately chosen coarser to avoid segregation of iron ore and coal mixture during fluidization. Three different types of coals, namely, Bhurkunda, Samla and Woodcoal were used in the present investigation to study the effect of coal reactivity on the reduction of iron ore.

To calculate the percent reduction in these cases a slightly different method was used than that in previous section. It may be noted that Eq. (5.1) assumes that the net weight change in the iron ore sample is due to the removal of oxygen only. In those reduction experiments in which coal and/or methane are used as reducing agents, carbon saturated sponge iron is likely to be formed. Therefore, the weight change in these cases is related to both the oxygen loss and carbon pickup. Hence, Eq. (5.1), as such is not valid in these cases. Since Eqs (5.2) and (5.3) are based on regression analysis of large amount of data generated using a variety of reactors employing different types of reducing agents, it is believed that these equations will also be applicable to our system. Hence, it should be possible to calculate percent reduction using these equations provided that metallization values are known.

Percent metallization values versus time plots for the

Bhurkunda and Samla coals are shown in Fig. 5.6. Percent metallization obtained by wood coal was very small, this was most likely due to the segregation of iron ore and coal during the fluidization. Segregation of ore and wood coal was also seen in the cold model FBR. Reduction results with wood coal are, therefore, not be plotted in Fig. 5.6. Further, it was seen that the Bhurkunda coal had higher reactivity than the Samla coal. Hence, all the subsequent experiments were carried out with Bhurkunda coal only. Fig. 5.7 shows percent total iron and percent metallic iron as a function of time. Corresponding percent metallization values are plotted in Fig. 5.8. It was possible to back calculate percent reduction knowing the percent metallization using the Eqs. (5.2) and (5.3). Percent reduction was also calculated using Eq. (5.1). These values are compared with those calculated using Eqs. (5.2) and (5.3) in Table 5.2. It is seen that percent reduction values calculated using Eq. (5.1) are lower than those obtained from Eqs (5.2) and (5.3). As mentioned above also, the percent reduction values calculated using Eqs. (5.2) and (5.3) are likely to be more accurate. Variation of these values with time is shown in Fig. (5.9).

Activation energy was calculated as described in the previous section. plots of $-\ln(1-\alpha)$ vs time are shown in Fig. 5.10 while 5.11 is a plot of $\ln(k)$ vs $\frac{1}{T}$. Activation energy calculated from the slope of the later figure is 40.0 kcal/mol. This value also falls within the range of 36-42 kcal/mol, as reported in literature (Table 2.2).

As stated earlier, reduction of iron oxide with coal may involve the following chemical reaction

$$Fe_2O_3 + 3C \longrightarrow 2Fe + 3CO \qquad (5.8)$$

$$Fe_2O_3 + 3CO \longrightarrow 2Fe + 3CO_2 \qquad (5.9)$$

$$C + CO_2 \longrightarrow 2CO \qquad (5.10)$$

It is known from the literature [34] that the activation energy of iron oxide reduction with CO is 28.1 kcal/mol while that for carbon gasification reaction is 86.0 Kcal/mol. Thus comparing our calculated values with these values it is evident that under the conditions used in the present investigation both the reduction of iron oxide with CO and carbon gasification reaction contribute to overall reaction kinetics.

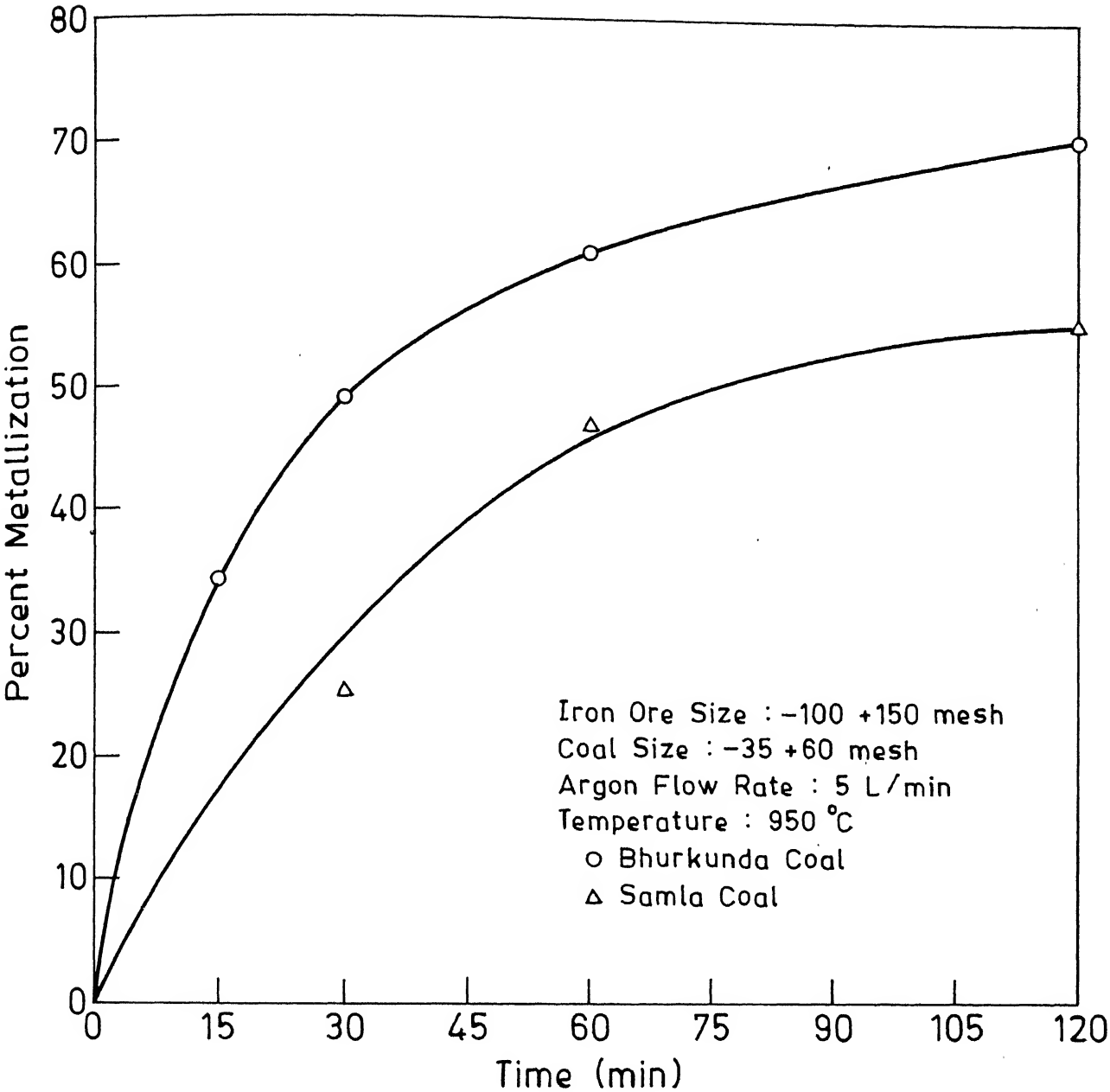

Figure 5.6: Plot of percent metallization as a function of time for two different coal.

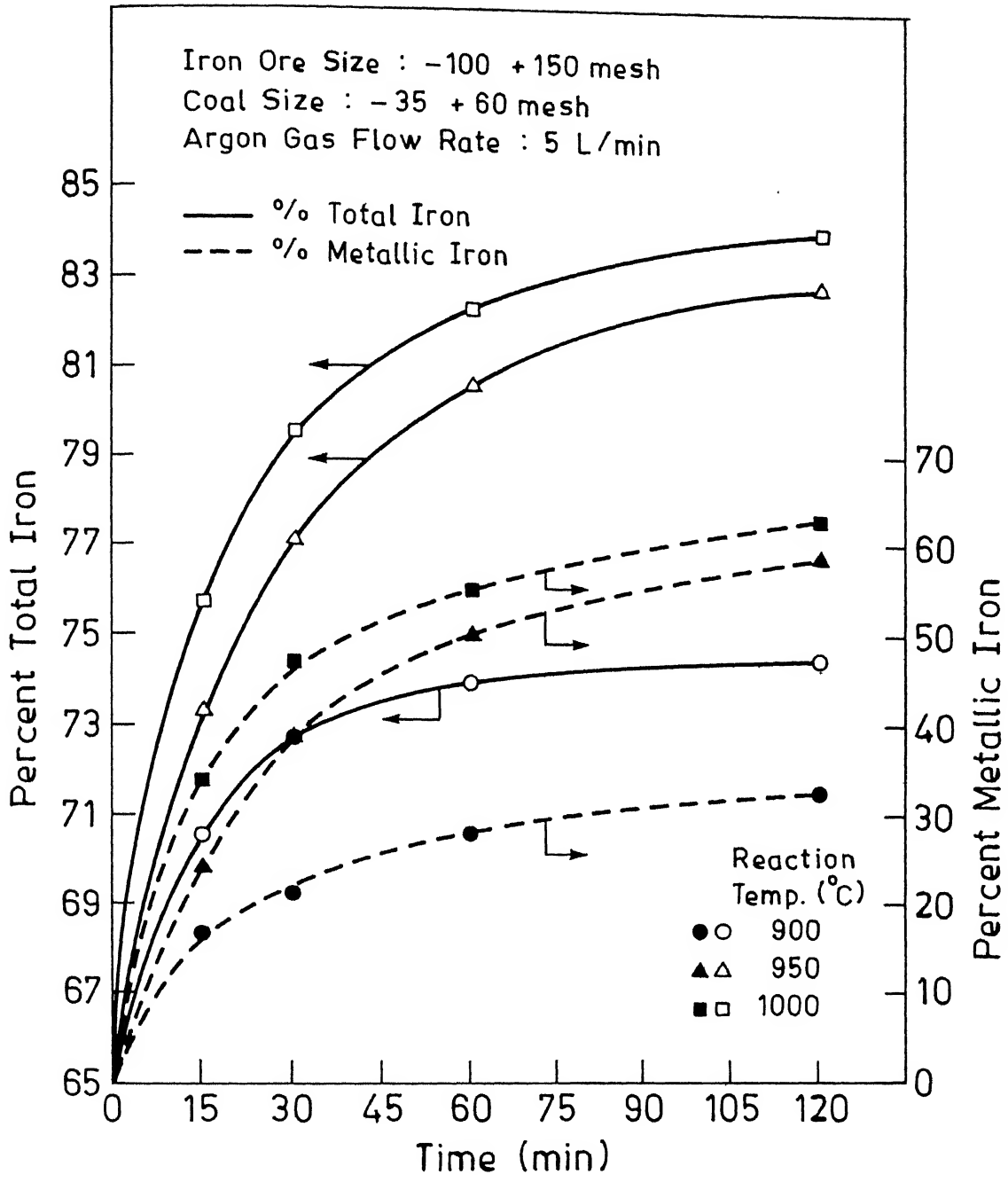

Figure 5.7: Plot of percent metallic iron and percent total iron in the reduced sample as a function of time at three temperatures in case of reduction with coal.

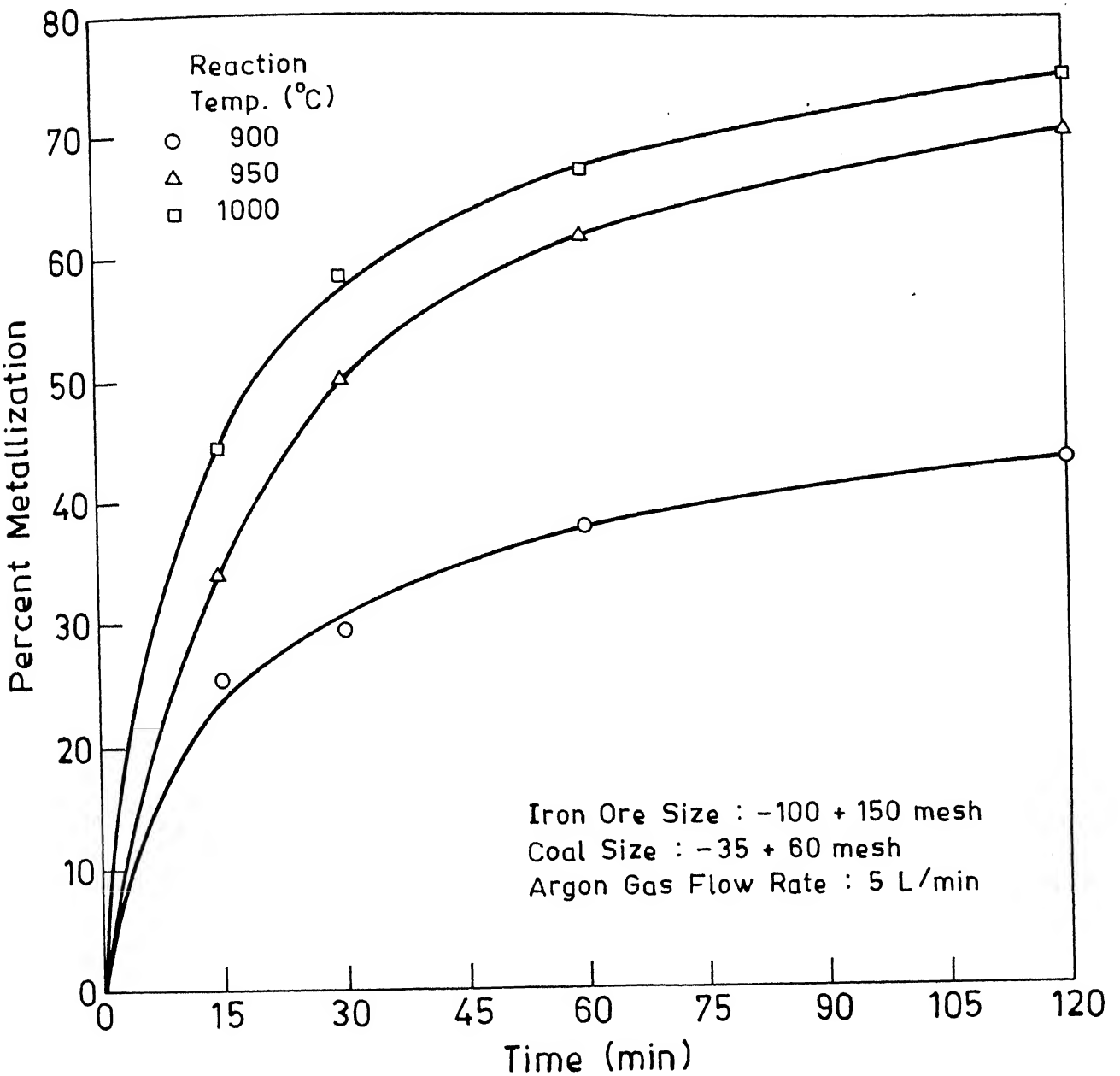

Figure 5.8: Plot of percent metallization as a function of time at three temperatures in case of reduction with coal.

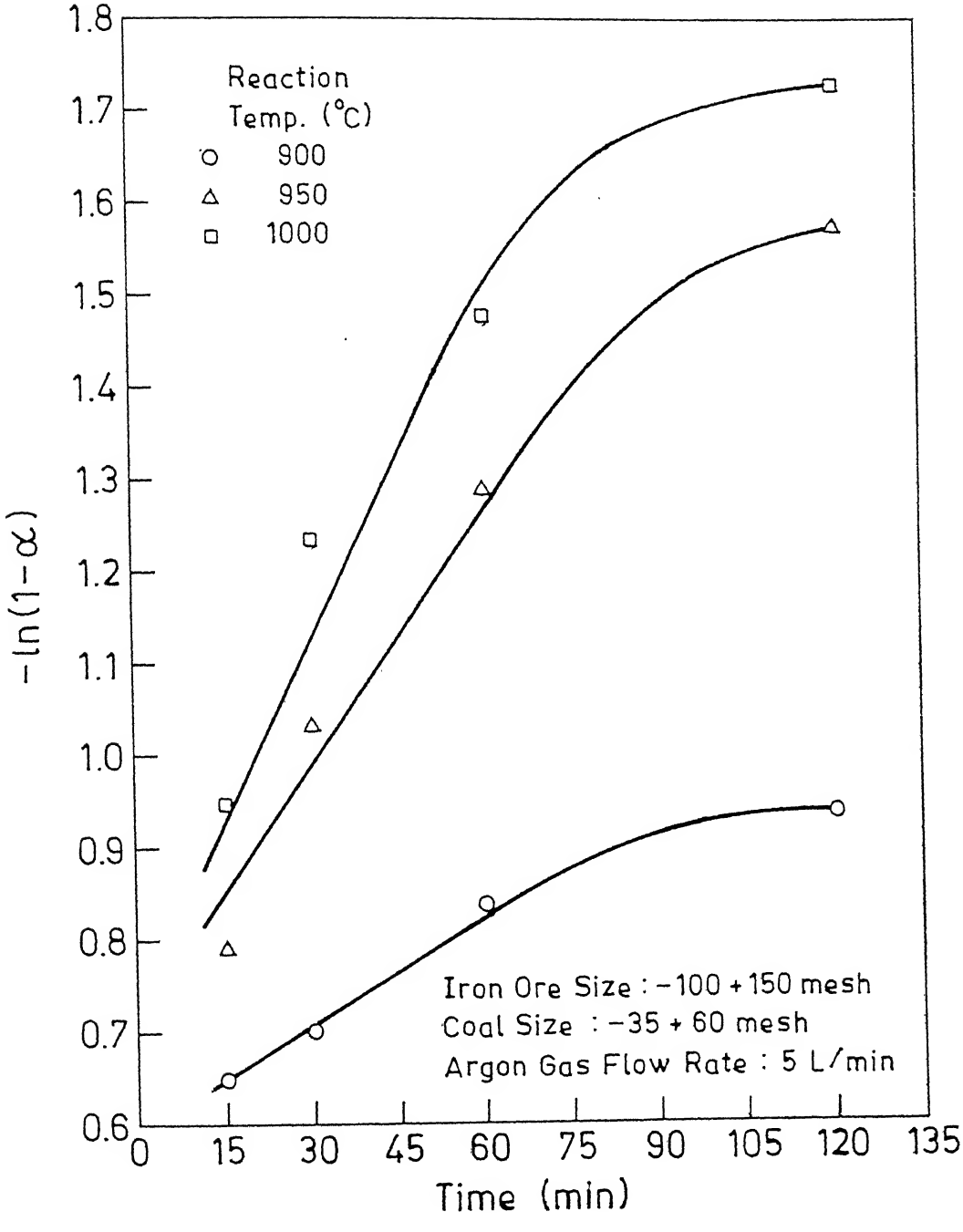

Figure 5.10: Plot of $-\ln(1-\alpha)$ as a function of time at three temperatures in

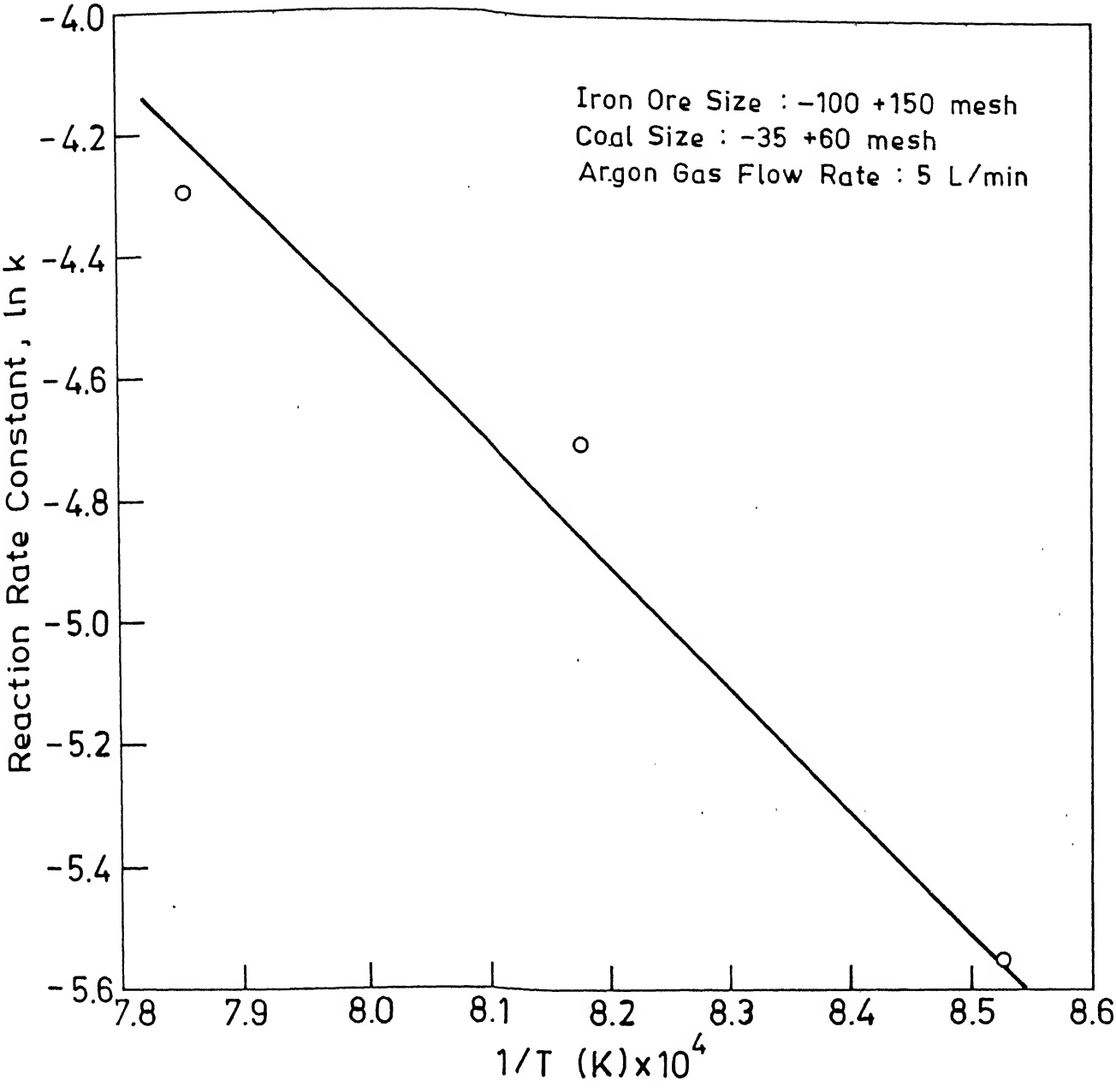

Figure 5.11: Plot of ln(k) as a function of reciprocal of temperature in case of reduction with coal.

Table 5.2 : Different experimental condition and obtained result of iron ore reduction with coal as a reducing agent

	t (min)	T (^{o}C)	$\%Fe_m$	$\%Fe_t$	$\%M_{ex}$	$\%R_{ex}$	%R
EC1	15	900	17.9	70.56	25.368	47.54	28.56
EC2	30	900	21.28	72.80	29.23	50.50	38.68
EC3	60	900	28.0	73.92	37.88	56.86	43.54
EC4	120	900	32.34	74.48	43.61	60.91	45.91
EC5	15	950	25.2	73.36	34.35	54.3	41.18
EC6	30	950	38.1	77.28	49.3	64.86	57.26
EC7	60	950	49.28	80.64	61.1	72.88	69.84
EC8	120	950	58.48	82.88	70.56	79.26	77.66
EC9	15	1000	33.6	75.88	44.28	61.38	51.7
EC10	30	1000	47.04	79.80	58.95	71.40	66.80
EC11	60	1000	55.44	82.32	67.35	77.10	75.75
EC12	120	1000	63.0	84.00	75.0	82.27	81.42
EC*13	30	950	16.0	71.96	22.23	45.06	34.92
EC*14	60	950	37.0	78.40	47.20	63.41	61.58
EC*15	120	950	45.0	80.64	55.80	69.29	69.84
EC**16	15	950	0.05	66.64	0.08	9.06	9.06
EC**17	30	950	0.08	67.20	0.116	11.97	11.97
EC6#	30	950	35.6	76.44	46.57	62.41	53.95

* Coal from Samla mines is used in this experiments

** Wood Coal is used in this experiments

Rest symbols are same as in the Table 5.3 # Repeated

5.3 Reduction of Iron Ore With Hydrogen and Methane Mixture

A few experiments were carried out using methane as a reducing agent. During the course of these experiments, the initial rate of reduction was found to be unexpectedly sluggish. Therefore, in the next series of experiments, hydrogen and methane mixture were used as reducing agents. Reaction temperature is varied between 900-1000^{o}C. Methane and hydrogen gas flow rates are kept 1.0 l/min each. Reduction time is varied between 15-60 minutes.

Fig.5.12 shows percent total iron and percent metallic iron as a function of time while Fig.5.13 shows the percent metallization as a function of time at three temperatures. Percent reduction was back calculated from the percent metallization data using Eqs (5.2) and (5.3). Percent reduction is also calculated from Eq.(5.1) and compared with those calculated from metallization as shown in Table 5.3. Fig.5.14 shows the percent reduction values (as obtained using Eqs 5.2 and 5.3) as a function of time.

Fig 5.15 shows the plots of $-\ln(1-\alpha)$ versus time. $\ln(k)$ vs $\frac{1}{T}$ is plotted in Fig 5.16. The activation energy calculated in this case was around 24.47 kcal/mol.

In the case of reduction with methane-hydrogen mixture, the chemical reactions involved are

$$CH_4 \longrightarrow C+2H_2 \qquad (5.11)$$

$$Fe_2O_3+2H_2 \longrightarrow 2Fe+3H_2O \qquad (5.12)$$

$$Fe_2O_3+3C \longrightarrow 2Fe+3CO \qquad (5.13)$$

$$Fe_2O_3+3CO \longrightarrow 2Fe+3CO_2 \qquad (5.14)$$

It is reported in literature that the activation energy for the reduction of iron ore with methane is in the range 48-52 kcal/mol (Table 3.3) and that the activation energy of iron ore with hydrogen is calculated to be 14.85 kcal/mol. Thus comparing our calculated value with these values it was evident that both the, reduction of iron ore with hydrogen and that with methane contributed to the overall reaction kinetics.

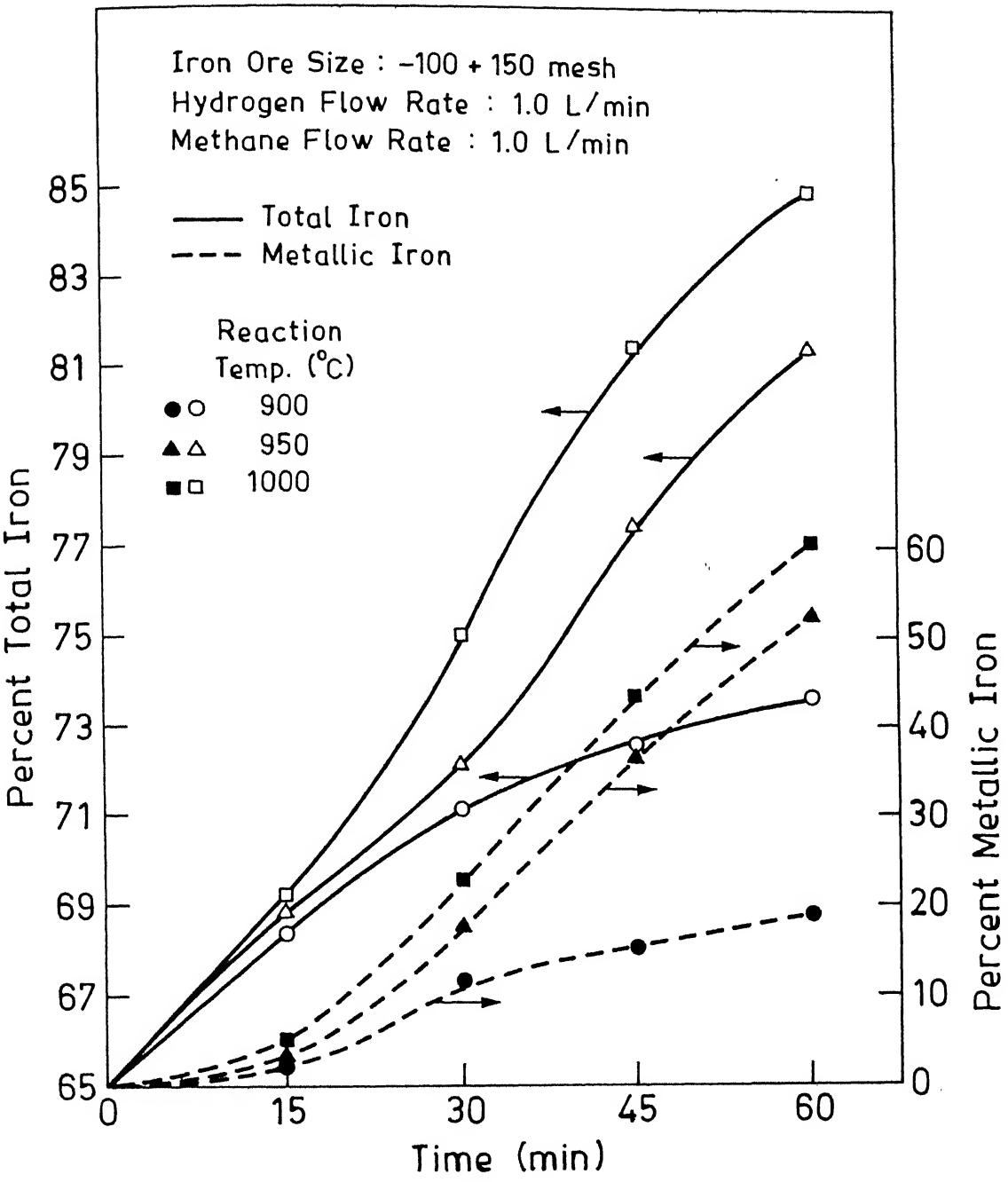

Figure 5.12: Plot of percent metallic iron and percent total iron in the reduced sample as a function of time at three temperatures in case of reduction with hydrogen and methane simultaneously.

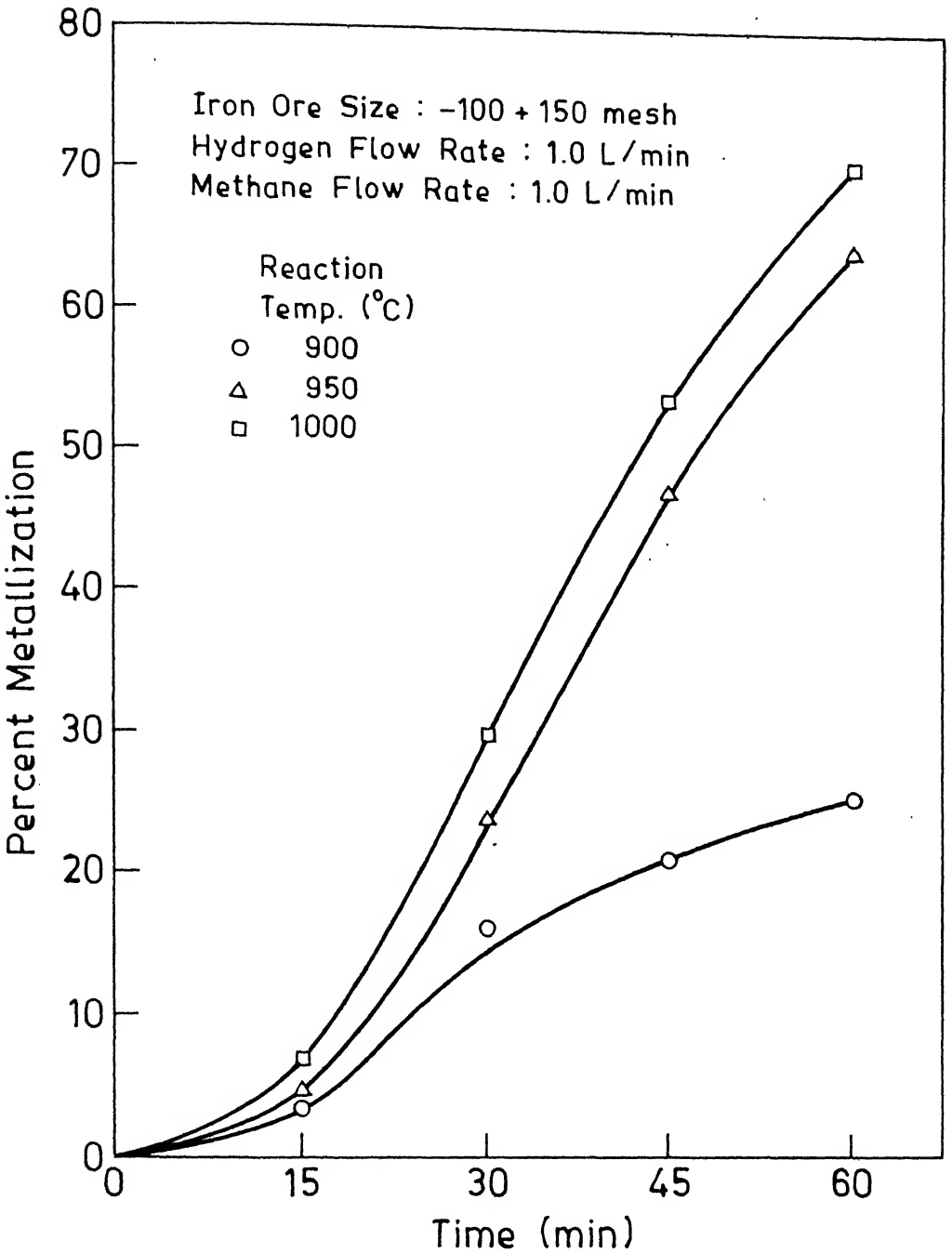

Figure 5.13: Plot of percent metallization as a function of time at three temperatures in case of reduction with hydrogen and methane.

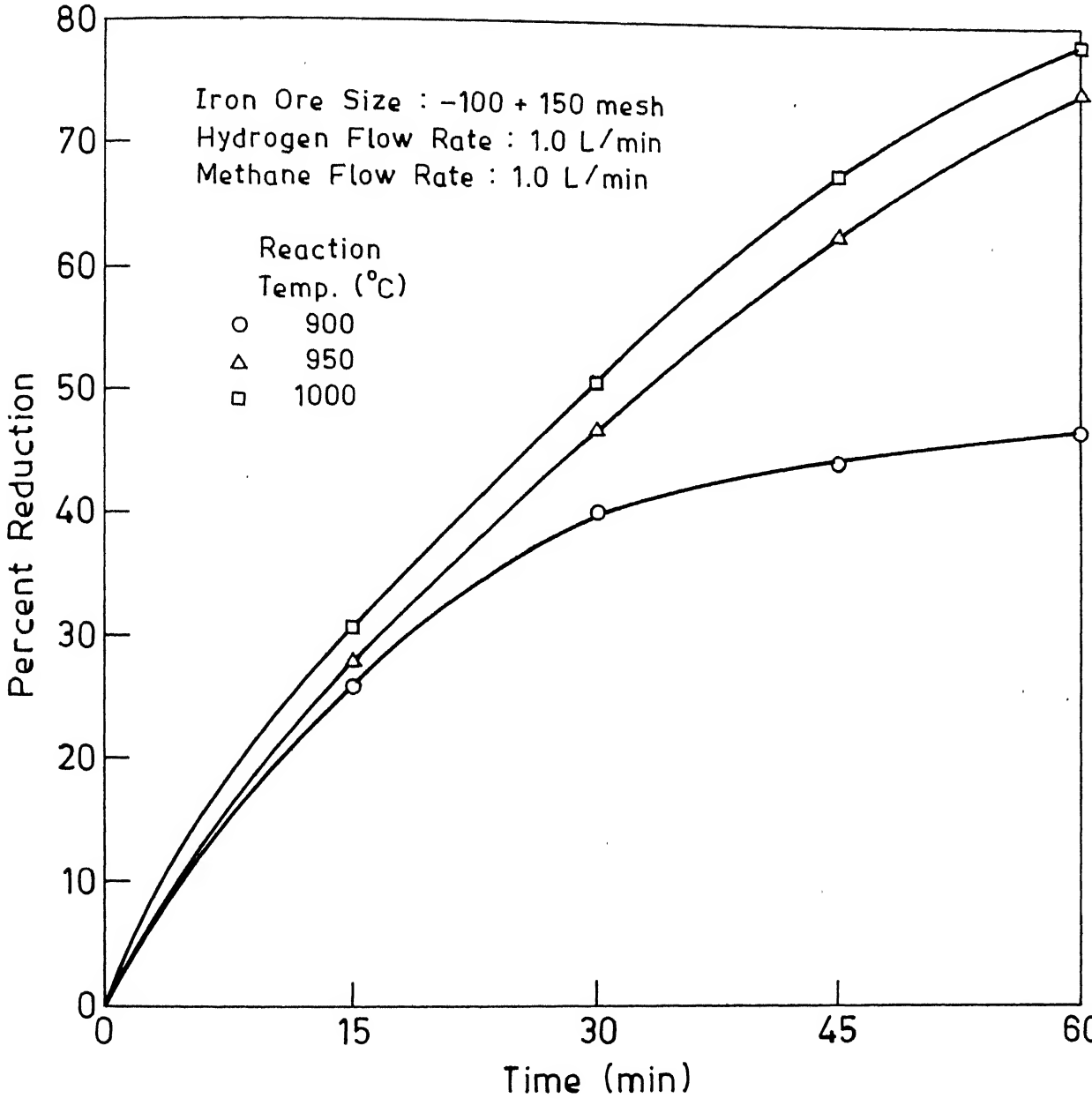

Figure 5.14: Plot of percent reduction as a function of time at three temperatures in case of reduction with hydrogen and methane.

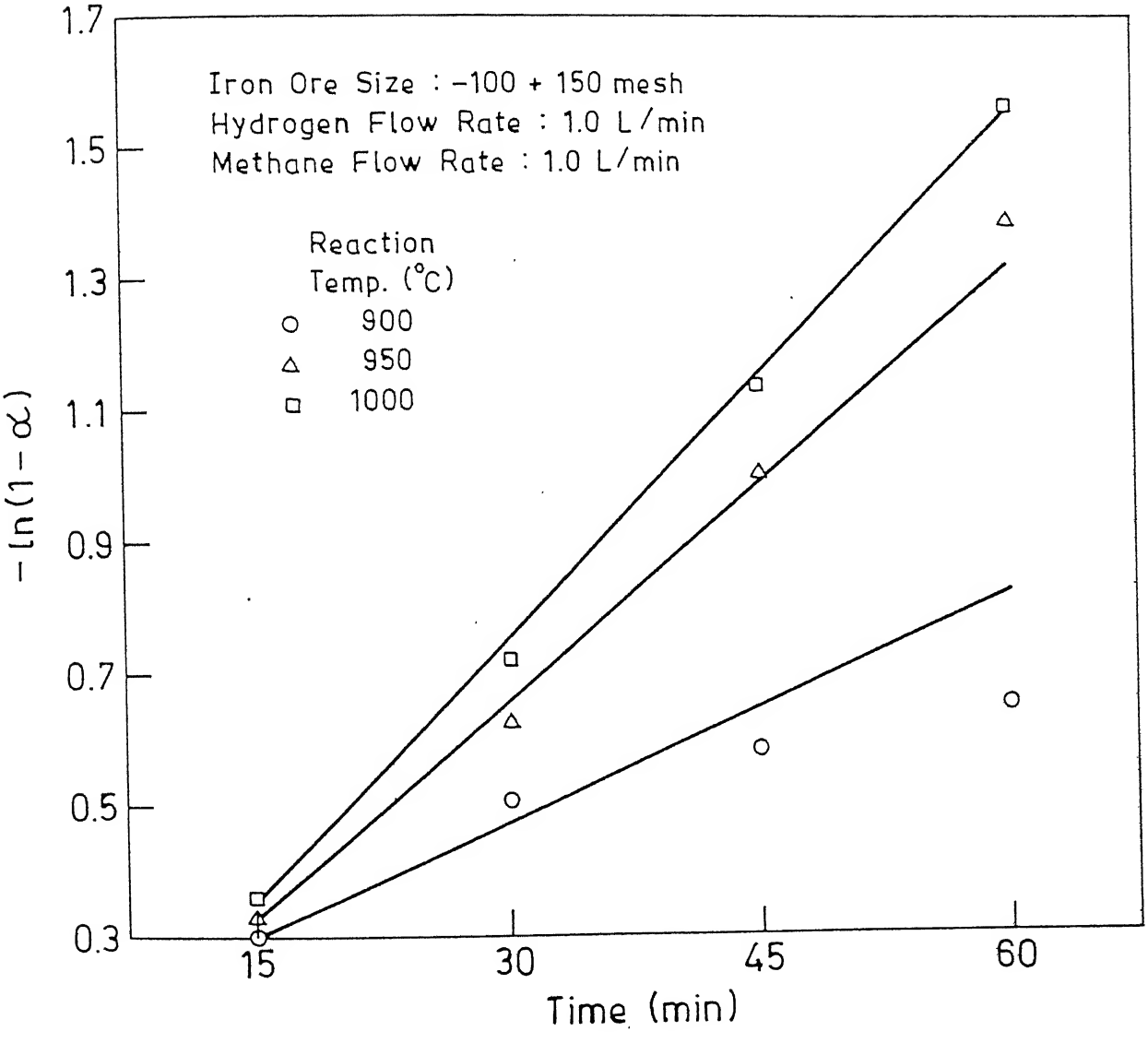

Figure 5.15: Plot of $-\ln(1-\alpha)$ as a function of time at three temperatures in case of reduction with hydrogen and methane

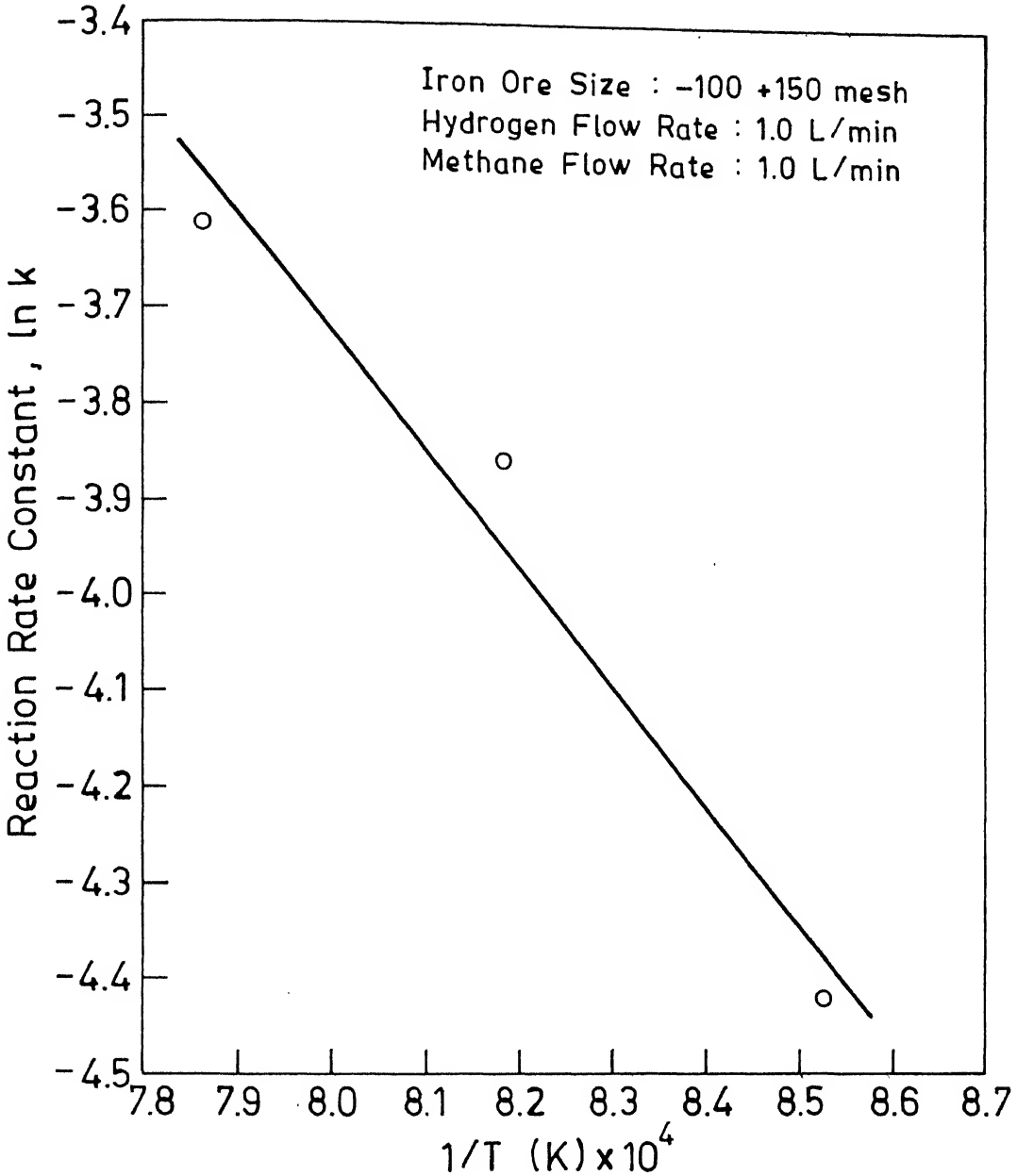

Figure 5.16: Plot of ln(k) as a function of reciprocal of temperature in case of reduction with hydrogen and methane simultaneously.

Table 5.3 : Different experimental condition and obtained result of iron ore reduction with methane and hydrogen as a reducing agent

	t (min)	T (^{o}C)	$\%Fe_m$	$\%Fe_t$	$\%M_{ex}$	$\%R_{ex}$	%R
EM* 1	15	900	-	66.08	-	-	6.09
EM** 2	30	950	-	66.36	-	-	7.58
EMH3	15	900	2.30	68.32	3.30	25.90	17.66
EMH4	30	900	11.76	71.12	16.53	40.10	31.11
EMH5	45	900	15.23	72.52	21.00	44.06	37.45
EMH6	60	900	18.82	73.64	25.50	47.68	42.34
EMH7	15	950	3.00	68.88	4.30	27.70	20.44
EMH8	30	950	17.60	73.08	24.08	46.50	39.91
EMH9	45	950	36.50	77.56	47.06	63.30	56.35
EMH10	60	950	52.50	81.48	64.43	75.10	72.82
EMH11	15	1000	4.50	70.00	6.40	30.90	25.86
EMH12	30	1000	22.50	75.04	30.00	51.07	48.24
EMH13	45	1000	43.68	81.20	53.79	67.93	71.80
EMH14	60	1000	60.50	85.96	70.38	79.14	87.75
EMH8#	30	950	19.04	73.64	25.86	47.98	42.34

*,** Experiments carried out with only methane as a reducing agent

t 1s the reduction time in minutes

Repeated

T is the reduction temperature in ^{o}C

$\%Fe_m$ is the percent of metallic iron in the reduced sample

$\%Fe_t$ is the percent of total iron in the reduced sample

$\%M_{ex}$ is the % metallization based on the experimental results

$\%R_{ex}$ is the percent reduction back calculated from Eqs 5.2 & 5.3

%R is the % reduction calculated from Eq. 5.1

5.4 Reduction Iron Ore With Coal and Methane Simultaneously

As mentioned above, an optimal process for producing sponge iron in a FBR in our country may be one in which iron ore is partially reduced with coal fines and partially with methane. To examine the feasibility of such a process, a number of experiments were carried out in this category at three temperature, namely, 900, 950 and 1000^{o}C. Reduction time was 15, 30, 45 and 60 minutes. Methane flow rate in all the experiments was 1.0 l/min. The amount of coal was stoichiometric (41.5 g).

Fig.5.17 shows percent total iron and percent metallic iron as a function of time in these various experiments. From this data, percent metallization was calculated and is shown in the Fig.5.18. Percent reduction as calculated from the percent metallization data using Eqs (5.2) and (5.3) is shown in Fig.5.19. Percent reduction, calculated from Eq. (5.1), is compared with that calculated from experimental metallization in Table 5.4.

Figures 5.20 and 5.21 are, respectively, the plots $-\ln(1-\alpha)$ vs t and $\ln(k)$ vs $\frac{1}{T}$, required for the activation energy calculation. Activation energy found to be 27.42 kcal/mol. Clearly, this value falls in between the activation energies for reduction with hydrogen (14.85 kcal/mol) and reduction with coal (40.0 kcal/mol). This suggests that the reduction of iron oxide with coal and methane mixture may be assumed a three step process. Initial reduction takes place with coal only. As metallic iron appears, it catalyzes the reformation of the methane into carbon and hydrogen in the second step. In the third step reduction of

iron oxide is primarily with hydrogen. It has been shown [42, 44] that methane is inert upto 30% reduction and only after some metallic iron is formed that it starts participating in the reduction reaction.

5.5 Characterization Of FBR Product Using X-Ray Diffraction

Characterization of iron ore as well as FBR product was done with the help of X-ray diffractographs. X-ray of as received iron ore showed clear peaks of Fe_2O_3 and traces of Fe_3O_4. A few samples of partially reduced iron ore with hydrogen were also subjected to X-ray. X-ray diffractographs of experimental samples EH9, EH6 in Table 5.1 clearly revealed the presence of metallic iron and small percent of wustite and traces of F_2O_3.

Some samples of the category EC were also examined to determine the carbon pickup. EC12 clearly shows some peaks of cementite, metallic iron and FeO. Previous investigator [52] had also confirmed the presence of cementite. However, detailed investigation of percent carbon were not possible in my case as the carbon determinator in our department was not functional.

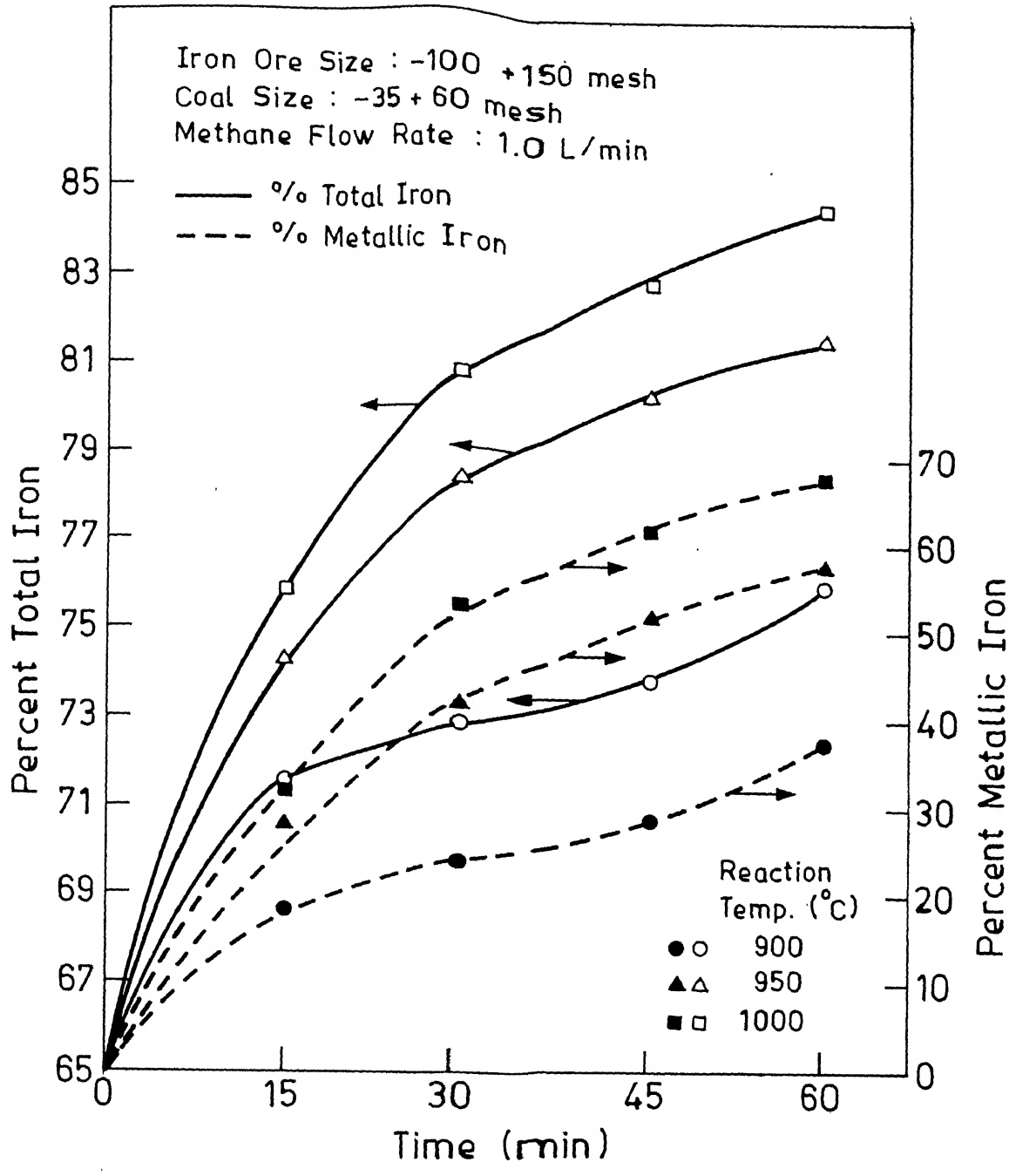

Figure 5.17: Plot of percent metallic iron and percent total iron in the reduced sample as a function of time at three temperatures in case of reduction with coal and methane simultaneously.

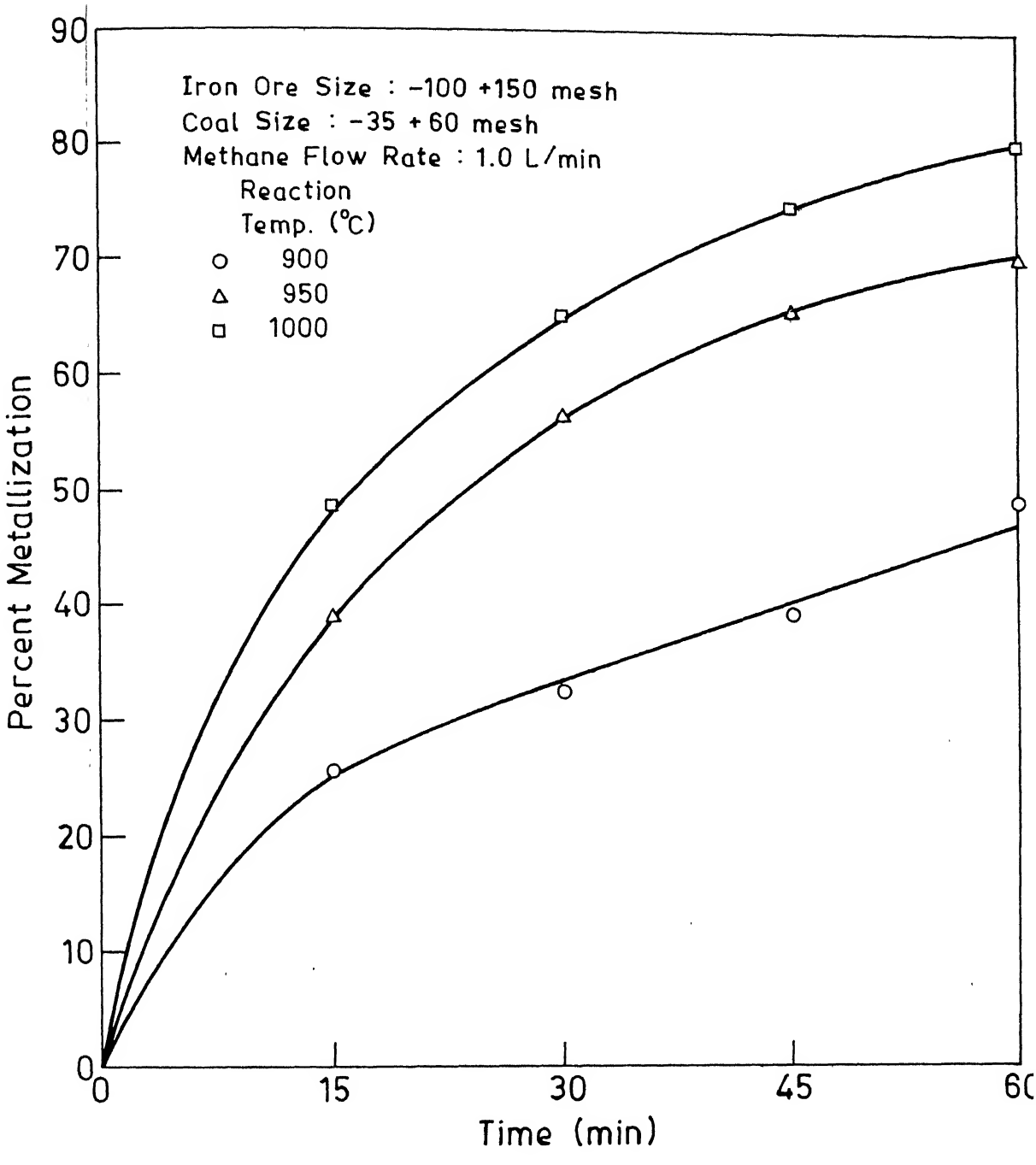

Figure 5.18: Plot of percent metallization as a function of time at three temperatures in case of reduction with coal and methane simultaneously.

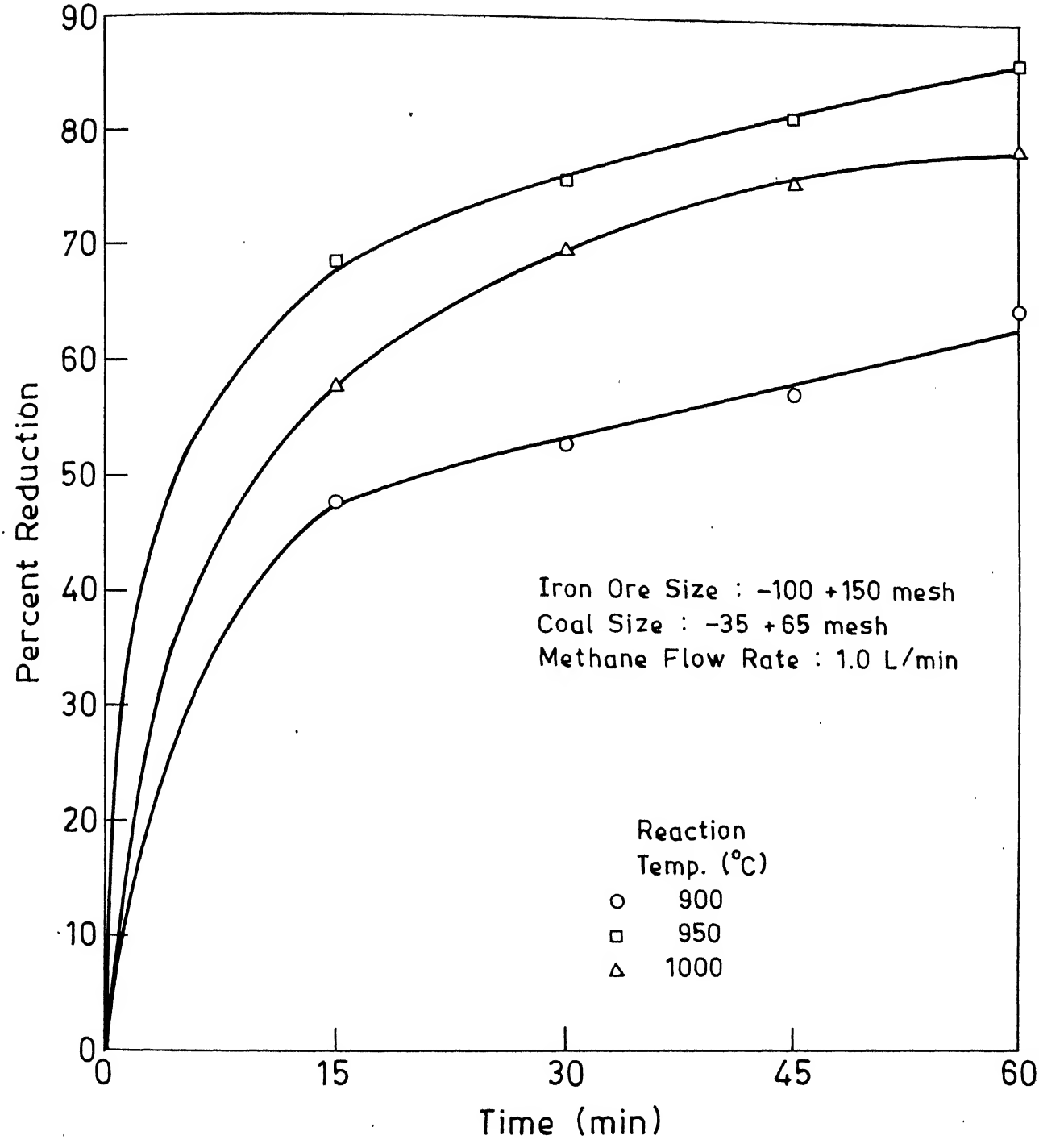

Figure 5.19: Plot of percent reduction as a function of time at three temperatures in case of reduction with coal and methane simultaneously.

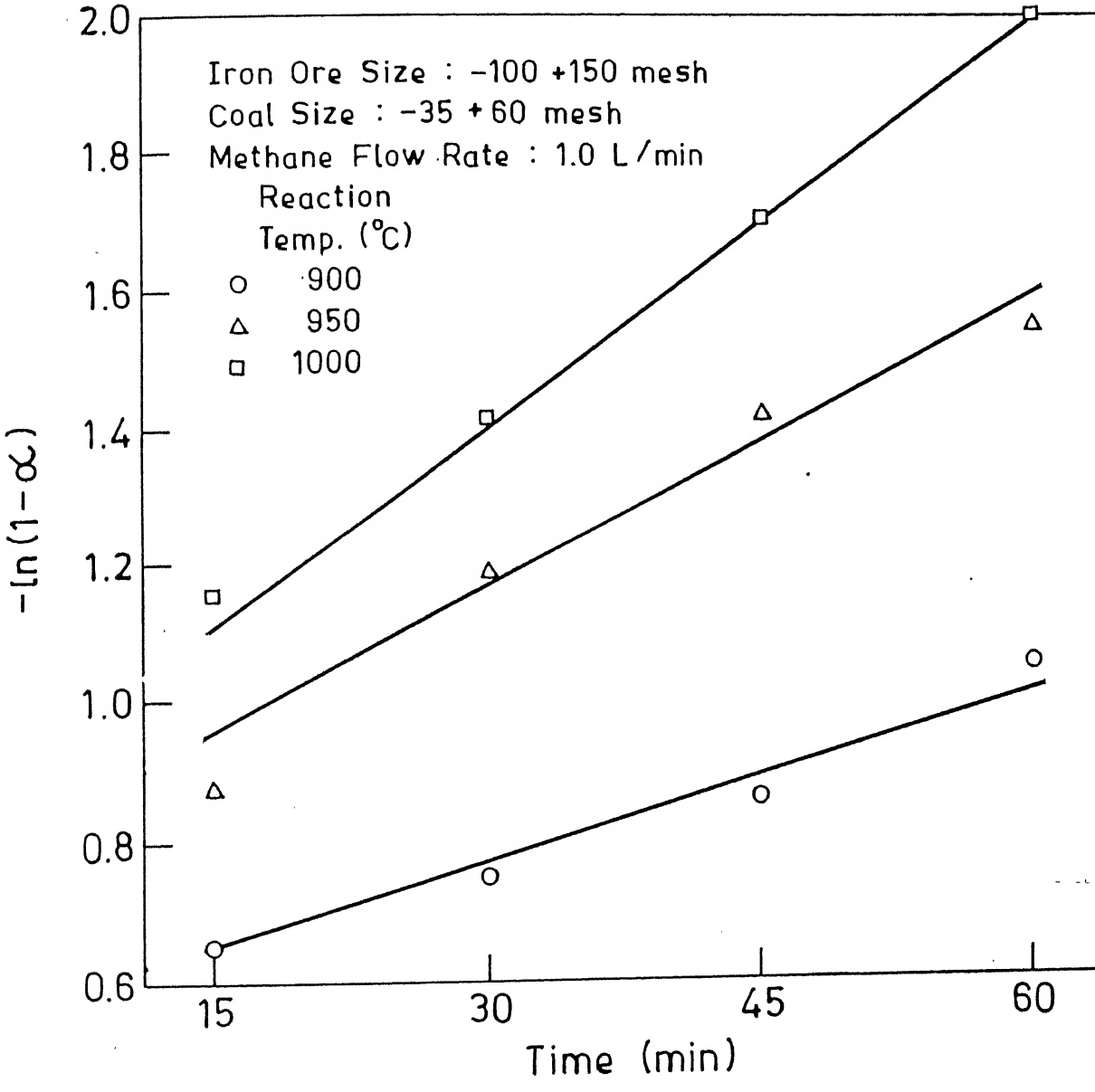

Figure 5.20: Plot of $-\ln(1-\alpha)$ as a function of time at three temperatures in case of reduction with coal and methane simultaneously.

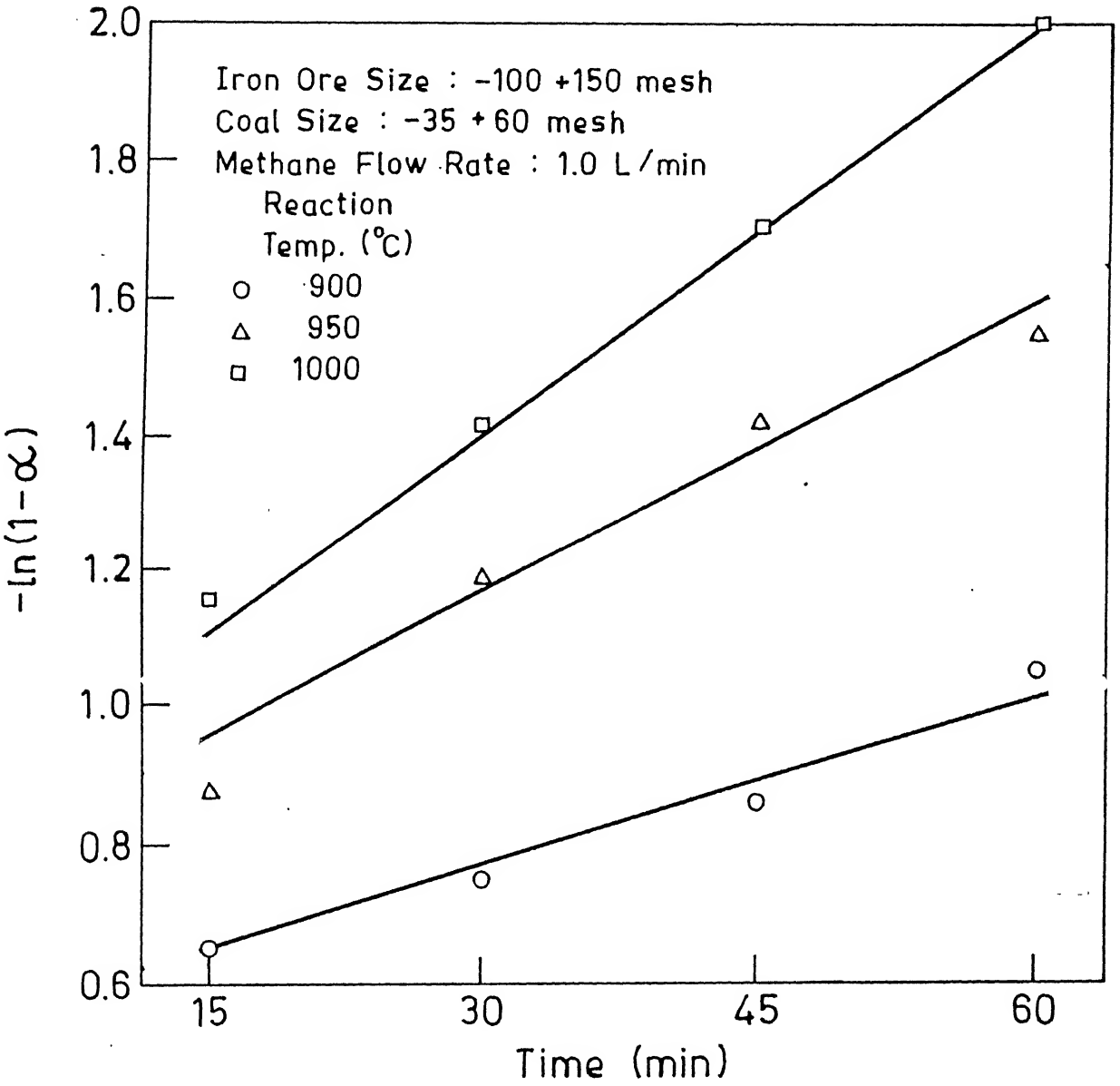

Figure 5.20: Plot of $-\ln(1-\alpha)$ as a function of time at three temperatures in case of reduction with coal and methane simultaneously.

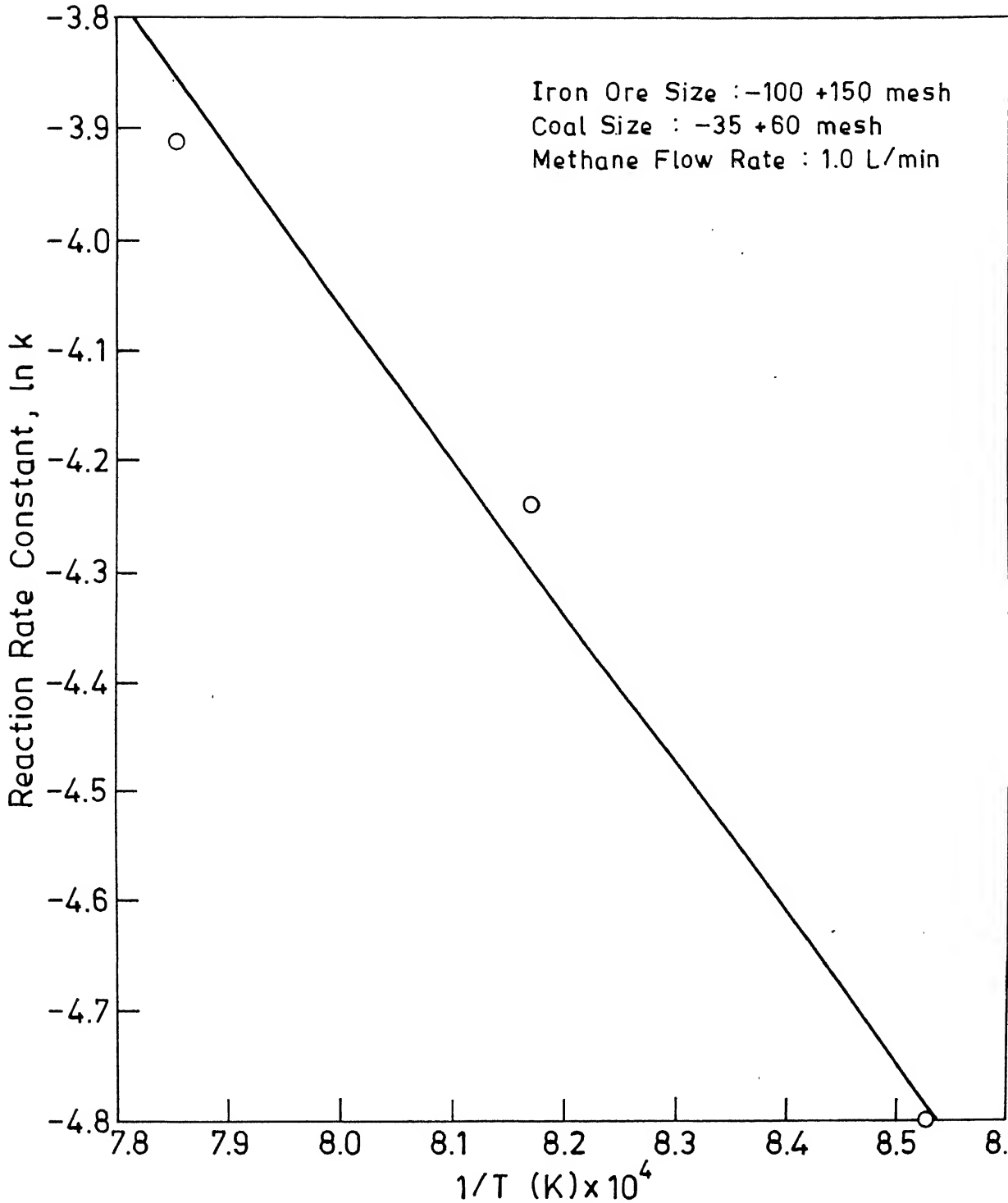

Figure 5.21: Plot of ln(k) as a function of reciprocal of temperature in case of reduction with coal and methane simultaneously.

Table 5.4 : Different experimental condition and obtained result of iron ore reduction with methane and coal as a reducing agent

	t (min)	T (^{o}C)	$\%Fe_m$	$\%Fe_t$	$\%M_{ex}$	$\%R_{ex}$	%R
EMC1	15	900	18.60	71.68	25.94	48.00	33.69
EMC2	30	950	23.52	72.80	32.30	52.80	38.68
EMC3	45	900	28.60	73.92	38.79	57.50	43.54
EMC4	60	900	38.00	76.16	49.89	65.27	52.82
EMC5	15	950	29.12	74.40	39.14	57.76	44.61
EMC6	30	950	44.25	78.40	56.44	69.73	61.58
EMC7	45	950	52.64	80.36	65.51	75.85	68.84
EMC8	60	950	57.24	81.76	70.01	78.88	73.81
EMC9	15	1000	37.00	75.88	48.76	63.49	51.69
EMC10	30	1000	52.88	80.92	65.35	75.75	70.84
EMC11	45	1000	61.75	82.88	74.50	81.90	77.66
EMC12	60	1000	68.32	84.84	80.35	86.06	84.17
EMC6#	30	950	48.5	79.24	61.20	70.39	64.73

t 1s the reduction time in minutes

T is the reduction temperature in ^{o}C

$\%Fe_m$ is the percent of metallic iron in the reduced sample

$\%Fe_t$ is the percent of total iron in the reduced sample

$\%M_{ex}$ is the % metallization based on the experimental results

$\%R_{ex}$ is the percent reduction back calculated from Eqs 5.2 & 5.3

%R is the % reduction calculated from Eq. (5.1)

CHAPTER 6

SUMMARY AND CONCLUSIONS

In the present investigation some basic aspects of reduction of iron oxide with different reducing agents in a high temperature FBR have been studied. With an objective to establish the feasibility of utilization of iron ore fines and coal fines directly for the production of carbon saturated sponge iron, four sets of experiments have been performed by changing reducing agents such as hydrogen, coal, hydrogen and methane mixture, coal and methane mixture. The process variables which have been examined during the course of this investigation are temperature, reduction time and reducing agent.

Sponge iron produced in FBR was chemically analyzed for total and metallic iron. From this data it could be possible to determine percent reduction as function of time. Reaction rate constants at various temperatures were calculated to calculate activation energy for various reducing agents using Arrhenius rate law. Characterization of FBR product was carried out by chemical in all reduced samples and X-ray analysis.

Following conclusions can be drawn from the present study.

1) The rate of reduction is highest for the reduction of iron ore with hydrogen. The overall activation energy in this case is around 14.85 kcal/mol while the value reported in literature

lies in the range of 10.87-19 kcal/mol. X-ray study of these samples showed presence of metallic iron as well as wustite.

2) Rate of reduction is slow when coal is used as a reducing agent due to solid-solid state reduction. But it can be increased by using a gaseous reductant along with coal. The overall activation energy for the reduction of iron ore with coal is around 40 kcal/mol. Reported activation energy values for coal are in the range of 36-42 kcal/mol. X-ray analysis of partially reduced samples reveal presence of cementite, metallic iron and wustite.

3) Rate of reduction is highly dependent upon the reactivity of coal. It was highest for the Bhurkunda coal.

4) Initial reduction rate is very sluggish when only methane is used as a reducing agent. It can, however, be increased by initiating the reduction with hydrogen and then methane as a reducing agent. The overall activation energy for the reduction of iron ore with hydrogen and methane mixture was found to be 24.47 kcal/mol.

5) Both iron ore fines and coal fines can be utilized in a FBR directly to produce carbon saturated sponge iron. However, Methane must be used as a reducing agent in the later stages of reduction for better production rate. Overall activation energy for the reduction of iron ore with coal and methane mixture was around 27.42 kcal/mol. Reduction of iron ore with coal and methane

simultaneously seems to be a three step process. In the first step iron ore is reduced by coal only. In the second step methane is reformed in hydrogen and carbon in the presence of metallic iron which acts as a catalyst. In the third step both coal and hydrogen take part in the reduction process leading to an increased reduction rate.

6.1 SUGGESTION FOR THE FUTURE WORK

1) Initially it was also planned to study the effect of particle size of iron ore as well as coal and reducing gas composition. We had programmed this investigation hoping that a gas chromatograph could be available and the kinetics of reduction of iron ore could be monitored by continuous analysis of out going gas. As there were major problems with the chromatograph in our laboratory. The same was not usable. Therefore, the entire experimental plan had to be changed. In the changed circumstances, the kinetics could be studied by carrying out reduction of a sample for a fixed time period and then taking out the sample and chemically analyzing the product. This not only increased the number of experiments substantially, but also added extra step of chemical analysis. Hence in the curtailed programme, effect of particle size, gas composition, etc could not be examined.

If the gas chromatograph can be made functional, extensive work can be done by analyzing the flue gas at different time intervals and effect of different parameters can be studied. In any future investigation on this subject, particle size of iron

ore as well as coal, gas composition can be varied to get a clear picture of reduction kinetics.

2) In the present set up there is no provision to take out samples from the FBR during the course of the reduction. An attempt may be made to modify the present set up so that samples may be taken out during the intermediate stages of the reduction.

3) Characterization of final product in the present study has been only preliminary. More rigorous characterization involving detailed X-ray and scanning electron microscopy may be desirable.

APPENDIX A

THEORETICAL ASPECTS OF FBR DESIGN

Fluidization is the operation by which fine solids are transformed in to a fluid like state through contact with a gas or liquid. This method of contacting has a number of unusual characteristics, and fluidization engineering is concerned with efforts to take advantage of this behavior and put it to good use. The following theoretical aspects of the subject are of utmost importance from the point of view of the design.

Pressure Drop Across a Fixed Bed [49, 50]

If a gas is passed through a bed of fine particles at a low flow rate, It merely percolates through the void spaces between stationary particles. This corresponds to a fixed bed situation. The pressure drop through a fixed bed of uniformly sized particles is given by Ergun [51]

$$\frac{\nabla p}{L} g_c = 150 \frac{(1-\varepsilon_m)^2}{\varepsilon_m^3} \frac{\mu u_o}{(\phi_s d_p)^2} + 1.75 \frac{1-\varepsilon_m}{\varepsilon_m^3} \frac{\rho_g u_o^2}{\phi_s d_p} \qquad (1)$$

where ∇p= Pressure drop across the bed (g-wt/cm^2)

L= length of bed (cm)

ε_m= Porosity of bed

ϕ_s= Shape factor

ρ_g= gas density (g/cm^3)

μ= Gas viscosity (g/cm sec)

d_p= particle size (cm)

g_c= Conversion factor (g(mass) cm/g-wt sec^2)

The pressure drop in Eq(1) represents two factors, the viscous and the kinetic energy losses. At low Reynolds number (Re_p<20), the viscous losses predominates and Eq(1) simplifies to

$$\frac{\nabla p}{L} g_c = 150 \frac{(1-\varepsilon_m)^2}{\varepsilon_m^3} \frac{\mu\, u_o}{(\phi_s d_p)^2} \qquad Re_p = \frac{d_p\ \rho_g\ u_o}{\mu} < 20 \qquad (2)$$

At high Reynolds number (Re_p>1000), the kinetic energy losses predominates and Eq(1) simplifies to

$$\frac{\nabla p}{L} g_c = 1.75 \frac{1-\varepsilon_m}{\varepsilon_m^3} \frac{\rho_g\ u_o^2}{\phi_s\ d_p} \qquad Re_p = \frac{d_p\ \rho_g\ u_o}{\mu} > 1000 \qquad (3)$$

In the intermediate range (20<Re_p<1000) Eq(1) is used. A schematic plot of Δp-u_o is shown in Fig. A.1.

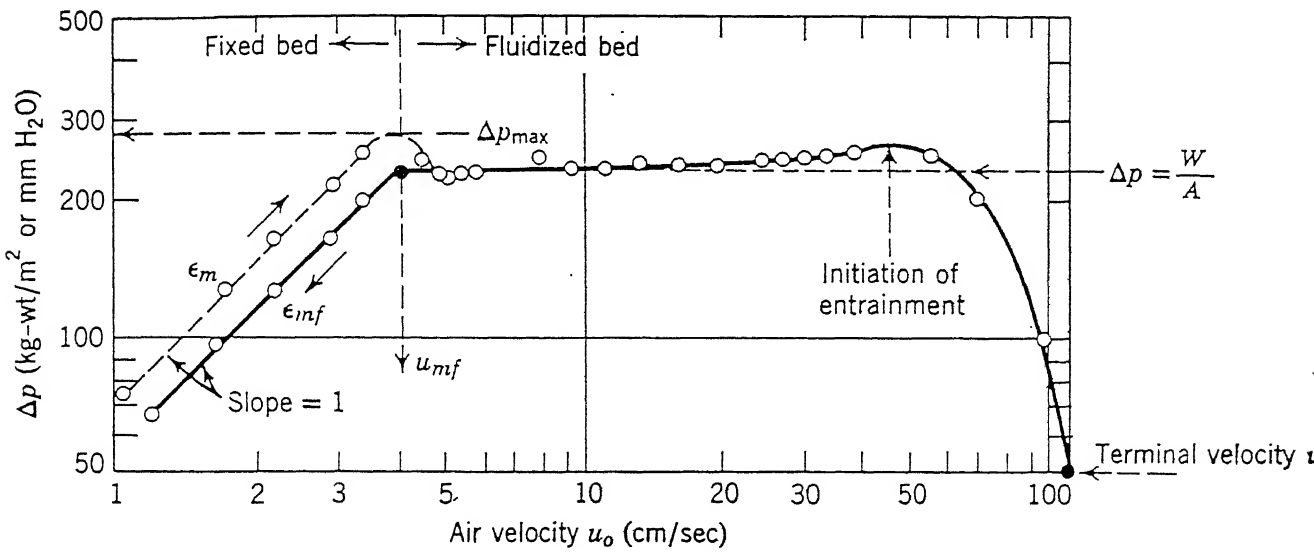

Figure A.1: Pressure drop vs velocity for a bed of uniformly sized particles

With an increase in gas flow rate, particles move apart and a few are seen to vibrate and move about in a restricted region. This state of bed corresponds to an expanded bed situation. At still higher velocities, a point is reached when the particles are all just suspended in the upward flowing gas. At this point the frictional force between a particle and gas counter balance the weight of the particle. This is called onset of fluidization.

Onset Of Fluidization

The onset of fluidization occurs when the drag force by upward moving gas is equal to the weight of bed

$$\left(\begin{array}{c}\text{drag force by}\\ \text{upword moving gas}\end{array}\right) = (\text{weight of particles})$$

or

$$\left(\begin{array}{c}\text{pressure drop}\\ \text{across bed}\end{array}\right)\left(\begin{array}{c}\text{cross}\\ \text{sectional}\\ \text{area of bed}\end{array}\right)=\left(\begin{array}{c}\text{volume}\\ \text{of bed}\end{array}\right)\left(\begin{array}{c}\text{fractions}\\ \text{of solids}\end{array}\right)\left(\begin{array}{c}\text{specific}\\ \text{weight of}\\ \text{solids}\end{array}\right) \quad (4)$$

or

$$\nabla P\, A_t = W = (A_t L_{mf})(1-\varepsilon_{mf})[(\rho_s - \rho_g)\frac{g}{g_c} \quad (5)$$

by arranging the terms

$$\frac{\nabla P}{L_{mf}} = (1-\varepsilon_{mf})(\rho_s-\rho_g)\frac{g}{g_c} \quad (6)$$

here the suffix mf shows the minimum condition of fluidization. The velocity corresponding to this state of bed is called minimum fluidization velocity.

Minimum Fluidization Velocity [49, 50]

Minimum fluidization velocity can be defined as that minimum

velocity which just renders the fixed bed fluidized. Following is the theoretical prediction of minimum fluidization velocity using the parameters such as particle size, particle density, gas viscosity, porosity etc. Combining Eq.(6) with Eq.(1) gives a quadratic equation in u_{mf}

$$\frac{1.75}{\phi_s \varepsilon_{mf}^3}\left(\frac{d_p\, u_{mf} \rho_g}{\mu}\right)^2 + 150\left(\frac{1-\varepsilon_{mf}}{\phi_s\, \varepsilon_{mf}^3}\right)\left(\frac{d_p\, u_{mf}\, \rho_g}{\rho}\right) = \frac{d_p^3\, \rho_g(\rho_s-\rho_g)g}{\mu^2} \qquad (7)$$

However, for small particles of small specific weight Eq.(1) simplifies to Eq.(2), thus Eq.(7) gives

$$u_{mf} = \frac{(\phi_s\, d_p)^2}{150}\left(\frac{\rho_s - \rho_g}{\mu}\right) g \left(\frac{\varepsilon_{mf}}{1-\varepsilon_{mf}^3}\right) \qquad Re_p < 20 \qquad (8)$$

For large particles Eq.(1) simplifies to Eq.(3) thus Eq.(7) gives

$$u_{mf}^2 = \frac{\phi_s\, d_p}{1.75}\left(\frac{\rho_s - \rho_g}{\rho_g}\right) g\, \varepsilon_{mf}^3 \qquad Re_p > 1000 \qquad (9)$$

If ε_{mf} and ϕ_s are unknown, the following empirical equations may be used [49, 50]

$$\frac{1}{\phi_s\, \varepsilon_{mf}^3} \cong 14 \qquad (10)$$

$$\frac{1-\varepsilon_{mf}}{\phi_s^2\, \varepsilon_{mf}^3} \cong 11 \qquad (11)$$

Using Eq.(10) and Eq.(11) in Eq.(7) equation for minimum fluidization velocity for different Reynolds numbers can be obtained.

$$u_{mf}=[(\frac{33.7\mu}{\rho_g d_p})^2 + 0.0408\frac{d_p(\rho_s-\rho_g)}{g}]^{0.5} - \frac{33.7\ \mu}{\rho_g\ d_p} \qquad (12)$$

or for small particles

$$u_{mf}=\frac{d_p^{\ 2}}{1650}(\frac{\rho_s-\rho_g}{\mu})g \qquad Re_p<20 \qquad (13)$$

or for large particles

$$u_{mf}^2=\frac{d_p}{24.5}(\frac{\rho_s-\rho_g}{\rho_g})\ g \qquad Re_p>1000 \qquad (14)$$

Terminal Velocity

The upper limit of the gas flow rate above u_{mf} is the terminal velocity u_t. The terminal velocity can be expressed in terms of drag coefficients as follows

$$u_t=\frac{4\ g\ d_p(\rho_s-\rho_g)}{3\ \rho_g\ C_d} \qquad (15)$$

For both spherical and non spherical particle, the terminal velocity u_t can be obtained from Fig A.2, an experimental correlation of the dimensionless group $C_dRe_p^2$ versus Re_p, where

$$Re_p=\frac{d_p\ \rho_g\ u_t}{\mu} \qquad (16)$$

and the velocity independent group

$$C_dRe_p^2=\frac{4\ g\ d_p^3\ \rho_g\ (\rho_s-\rho_g)}{3\ \mu^2} \qquad (17)$$

u_t can be determined by determining $C_dRe_p^2$ from known values of d_p, ρ_s, $\rho_g$and μ. The gas flow rate through a FBR is limited by two quantities, u_{mf} on one hand and u_t on other. These two are the

most important factor which influence the design of the FBR. To avoid carry over of fine particles from FBR, the velocity of gas should be in between the terminal velocity and minimum fluidization velocity.

$$u_{mf} < u_{op} < u_t$$

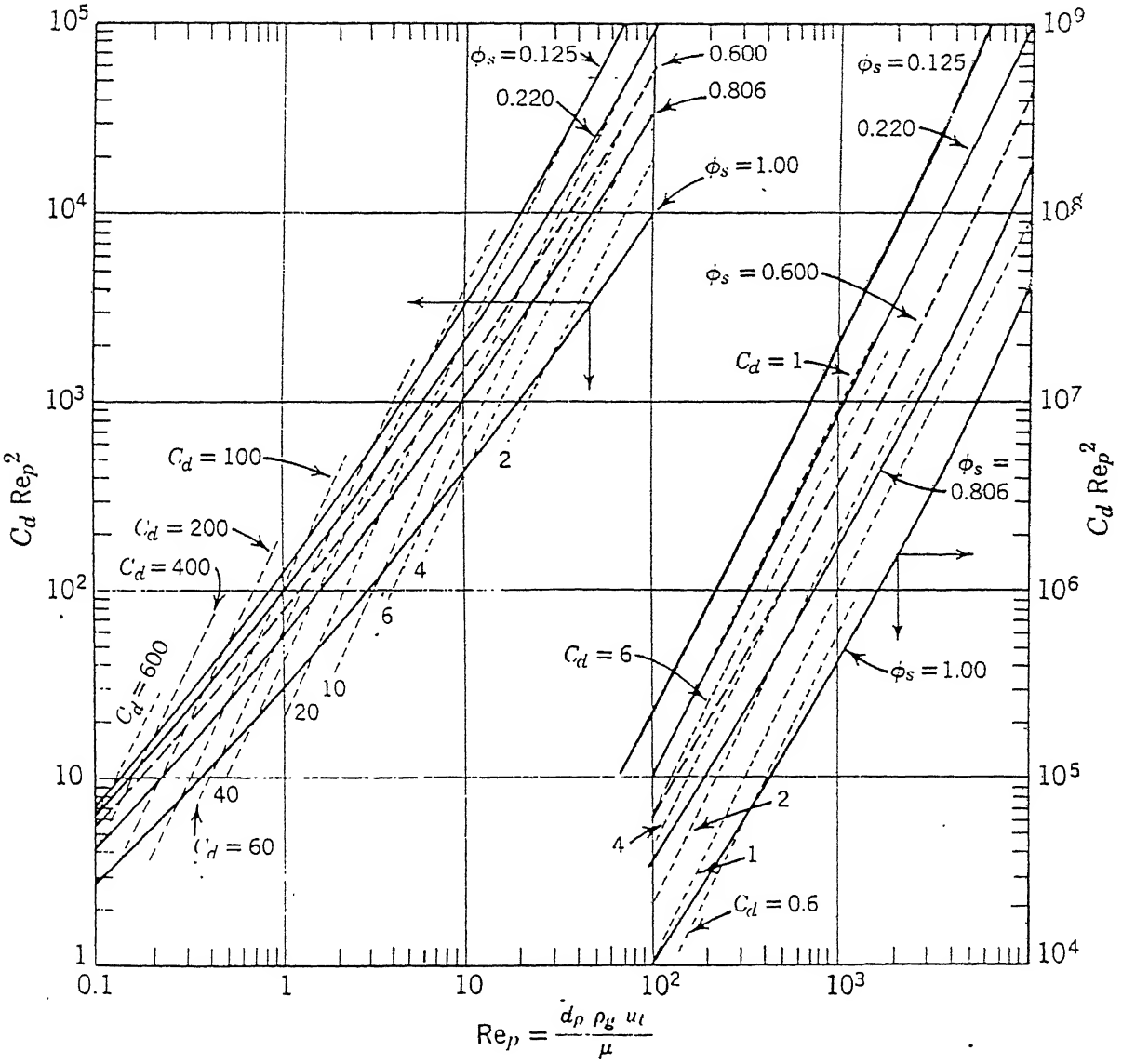

Fig. A.2: Plot for calculating the terminal velocity of particles

Distributor Design[49, 50]

The most important design parameter is the design of distributor plate. This is because the distributor influences the quality of fluidization to the greatest extent than any other parameter as shown in Fig. A.3. It is experimentally established that , larger the number of pores/holes in the distributor, better will be the quality of fluidization. Further , to ensure uniform gas flow through all openings of the distributor plate, the pressure drop across it should be 10% of the pressure drop across the bed.

$$P_{d\ min} = \max\ [0.1\ P_{bed}] \qquad (18)$$

For a fixed, maximum bed height, P_{bed} can be calculated from Eq.(2) or Eq.(3) and hence P_d can be calculated from Eq.(18). Once the superficial velocity (u_o) of the gas is known it is possible to calculate Reynolds number which then can be used to calculate the drag coefficient from Fig A.4. The velocity of gas through an orifice (u_o) can be calculated using the following Eq.

$$u_{or} = C_d^{'}\left(\frac{2g_c\ P_d}{g}\right)^{0.5} \qquad (19)$$

Knowing u_{or}, the number of pores per unit area (N_{or}) of the distributor plate can be calculated.

$$\frac{u_o}{u_{or}} = \frac{\pi}{4} d_{or}^2\ N_{or} \qquad (20)$$

Faulty design of the distributor or FBR results in a number of problems causing defluidization and making continuous operation impossible. Slugging and channelling are some of the problems related with the distributor plate.

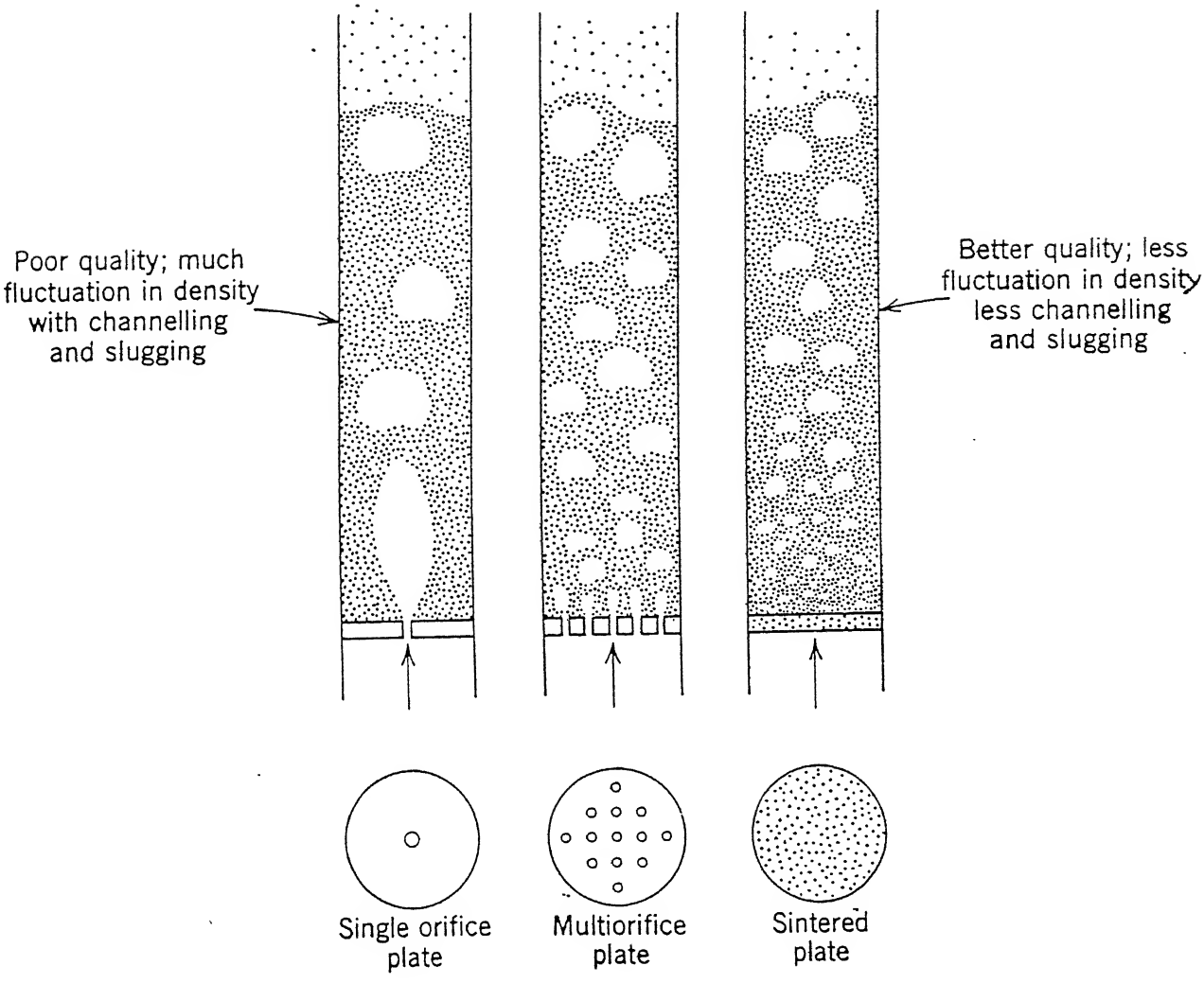

Figure A.3: Quality of fluidization as influenced by type of gas distributor

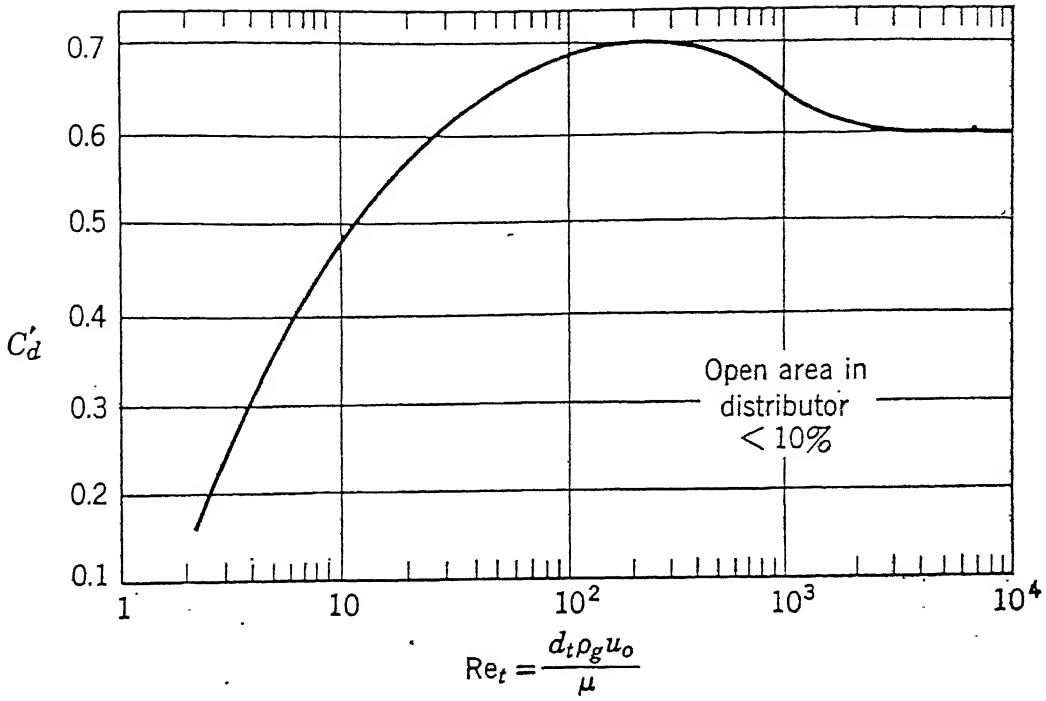

Figure A.4 : Orifice coefficient vs Reynolds number plot

Channelling

Channelling in fluidized bed reactor occurs when the pores in the distributor plate are too large or when there is sticking of particles at some parts of the bed. This also occurs when particle size is not uniform.

Slugging

It occurs when the bed is too long due to the coalescence of bubbles forming large bubble, of the size of reactor itself.

The pressure drop vs velocity diagram of FBR are very helpful when the fluidization phenomenon can not be observed visually in a rector. The diagram in Fig A.5 are examples of poorly fluidized beds. The large pressure fluctuation in Fig A.5.a suggest slugging bed, whereas an absence of the characteristic sharp change in slope at minimum fluidization and abnormally low pressure drop in Fig A.5.b suggest incomplete contacting with particles i.e. channelling.

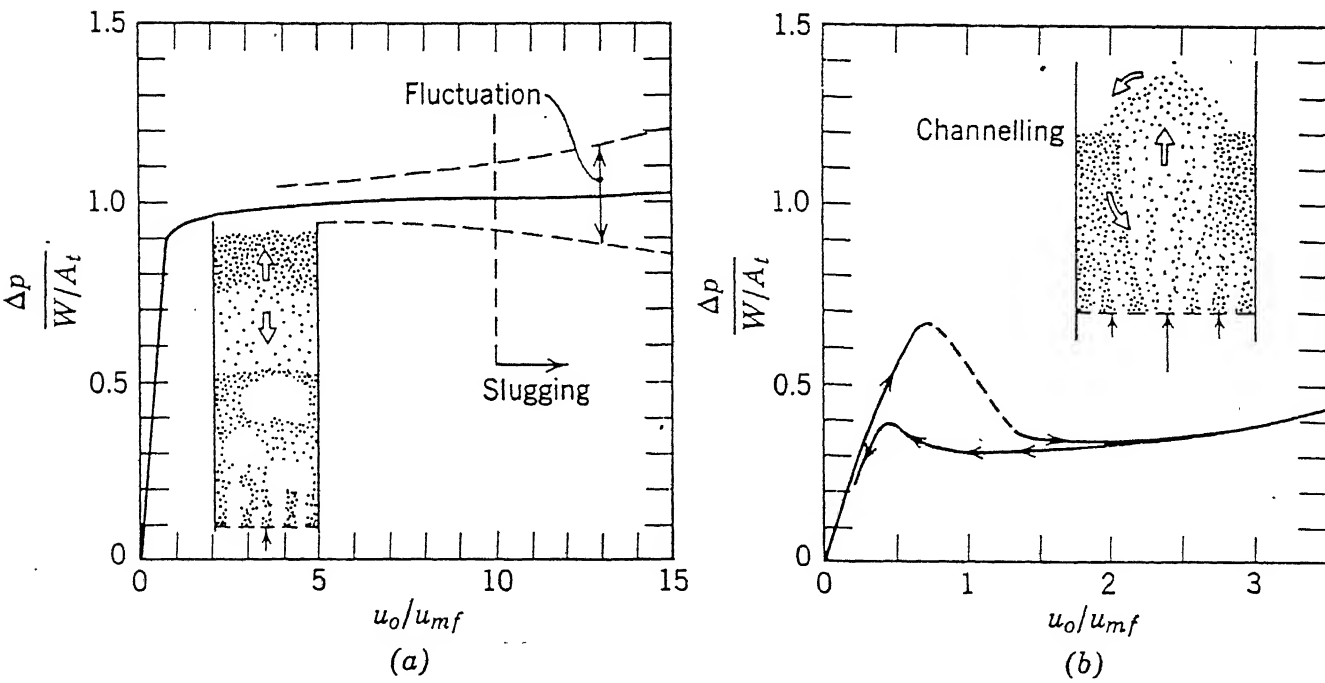

Figure A.5 : Pressure drop diagram for poorly fluidized beds

APPENDIX B

DERIVATION OF PERCENT REDUCTION EQUATION SUGGESTED BY GONZALES[48]

If W_i is the initial mass of the sample and W_f is the final weight of the sample after reduction. From the mass balance

$$W^i(\%Fe)_t^i = W^r(\%Fe)_t^r$$

$$(\%Fe)_t^r = (W^i/W^r)(\%Fe)_t^i$$

$$(\%Fe)_t^r = \left(\frac{1}{1-\nabla W}\right)(\%Fe)_t^i \qquad (1)$$

where ∇W = the fractional loss in the initial sample

$(\%Fe)_t^i$ = Percent of total iron in the initial iron ore

$(\%Fe)_t^r$ = Percent of total iron in the reduced iron ore

∇W can also be defined as

$$\nabla W = \left[\frac{\%R\ (\%O_2)^i}{100\times100}\right] \qquad (2)$$

where %R is the percentage of reducible oxygen removed from the initial ore and $(\%O_2)^i$ is the percent oxygen in the initial sample in form of iron oxide.

Substituting the value of ∇W from Eq.(2) to Eq.(1)

$$(\%Fe)_t^r = \left[\frac{1}{1 - \left[\frac{\%R\ (\%O_2)^i}{100\times100}\right]}\right](\%Fe)_t^i$$

$$1-\left[\frac{\%R\ (\%O_2)^i}{100\times100}\right]=\frac{(\%Fe)_t^i}{(\%Fe)_t^r}$$

$$\left[\frac{\%R\ (\%O_2)^i}{100\times100}\right]=1-\frac{(\%Fe)_t^i}{(\%Fe)_t^r}$$

$$\%R=\left[\frac{(\%Fe)_t^r-(\%Fe)_t^i}{(\%Fe)_t^r}\right]\frac{100\times100}{(\%O_2)^i} \qquad (3)$$

Percent $(\%O_2)^i$ in terms of $(\%Fe)_t^i$ can be defined as

$$(\%O_2)^i=(112/48)\times(\%Fe)_t^i \qquad (4)$$

Substituting the value of $(\%O_2)^i$ from Eq.(4) to Eq.(3)

$$\%R=(112/48)\times\left[\frac{(\%Fe)_t^r-(\%Fe)_t^i}{(\%Fe)_t^r\times(\%Fe)_t^i}\right]\times10000$$

REFERENCES

1) Annual Report of CSLS, Central Fuel Research Institute, Bihar, India, 1982

2) Fukunaka Y., Monta T. and Asaki Z. and Kondo Y., Met.Trans., 7B(1976)307

3) Doheim M.A., Abdil-Wahab M.Z. and Rassoul S.A., Met.Trans., 7B(1976)477

4) Natesan K. and Philbrook W.O., Met.Trans., 1B(1970)1353

5) Evans J.W., Song S. and Leon-Sucre C.E., Met.Trans., 7B(1976)55

6) Habasi F., Progresses in Extractive Metallurgy, Golden and Breach Publisher, vol 1, 21-93

7) Gutierrez L.A. and Watkinson A.P., Fuel, 61(1982)133

8) Agrawal B.B., Bandopadhyay A. and Prasad K.K., Progress in Met. Research Fund. and Appl. Aspects, Feb 1985, IIT Kanpur

9) Joseph T.L., Trans AIME, 120(1936)72

10) Udy M.C. and Lorig C.H., Trans AIME, 154(1943)154

11) Bagdandy L.V. and Janke W., Z. Elektrochem, 61(1957)1147

12) McKewan W.M., Transcation of The Metallurgical Society of AIME, 218(1960)2

13) Turkdogan E.T. and Vinters J.V., Met. Trans, 2(1971)3175

14) Turkdogan E.T. and Vinters J.V., Met. Trans, 2(1971)3189

15) Turkdogan E.T. and Vinters J.V., Met. Trans, 3(1972)1561

16) Ezz S.Y., Transcation of The Metallurgical Society of AIME, 218(1960)709

17) Hutchings K.M.,Smith J.D., Yoruk S. and Hawkins R.J., Ironmaking and Steelmaking, 14(1987)103

Steelmaking, 18(1991)211

40) Nixon I.G., Ironmaking and Steelmaking, 7(1980)2

41) Ghosh D., Roy A.K and Ghosh A.K., Trans ISIJ, 26(1986)186

42) Hutchings K.M., Hawkins R.J. and Smith J.D., ironmaking and Steelmaking, 15(1988)121

43) Barrett D., Ind. Eng. Chem. Process Des. Develop., 11(1972)415

44) Ruprecht P. and Baerns M., Chem Eng Tech, 43(1971)894

45) Direct Reduction of Iron Ore, a bibliographical survey, The Metals Society, London, 1979

46) Stephenson R.L. and Smailer R.M., Direct Reduced Iron, The Iron and Steel Society of AIME, Warrendele, 1980

47) Kumar B.V., M.Tech Thesis, I.I.T.Kanpur, India, 1984

48) Dam Gonzales O.G. and Jeffes J.H.E., Ironmaking and Steelmaking, 14(1987)217

49) Davidson J.F. and Harrison D., Fluidization, Academic Press, NewYork, 1977

50) Ergun S., Chemical Engineering Prog., 48(1952)89

51) Kunii D. and Levenspiel O., Fluidization Engineering, John Wiley & Sons Inc, NewYork, 1969

52) Kumar B., M.Tech Thesis, I.I.T.Kanpur, India, 1987

A121705

A121705

Date Slip

This book is to be returned on the date last stamped.

MMF-1995-M-GOP-PRO